UNIVERSIDADE FEDERAL DE MINAS GERAIS
INSTITUTO DE CIÊNCIAS BIOLÓGICAS
Departamento de Botânica
Programa de Pós-Graduação em Biologia Vegetal

PPGBV
UFMG

UFMG

Arthur de Barros Rates

ALUMINUM AND SILICON INDUCED CHANGES IN ROOT CELL WALL COMPOSITION AND STRUCTURE OF *ZEA MAYS* L.

Dissertação apresentada ao Programa de Pós-Graduação em Biologia Vegetal do Departamento de Botânica do Instituto de Ciências Biológicas da Universidade Federal de Minas Gerais, como requisito parcial à obtenção do título de Mestre em Biologia Vegetal.

Área de Concentração Fisiologia Vegetal e Ecologia

Belo Horizonte – MG

2022

Arthur de Barros Rates

ALUMINUM AND SILICON INDUCED CHANGES IN ROOT CELL WALL COMPOSITION AND STRUCTURE OF *ZEA MAYS* L.

Versão final

Dissertação apresentada ao Programa de Pós-Graduação em Biologia Vegetal do Departamento de Botânica do Instituto de Ciências Biológicas da Universidade Federal de Minas Gerais, como requisito parcial à obtenção do título de Mestre em Biologia Vegetal.

Orientador: Prof. Dr. Marcel Giovanni Costa França

Belo Horizonte

2022

043 Rates, Arthur de Barros.
Aluminum and silicon induced changes in root cell wall composition and structure of Zea mays L. [manuscrito] / Arthur de Barros Rates. – 2022.
55 f. : il. ; 29,5 cm.

Orientador: Prof. Dr. Marcel Giovanni Costa França.
Dissertação (mestrado) – Universidade Federal de Minas Gerais, Instituto de Ciências Biológicas. Programa de Pós-Graduação em Biologia Vegetal.

1. Teoria da Densidade Funcional. 2. Parede Celular. 3. Pectinas. 4. Alumínio. 5. Silício. 6. Imuno-Histoquímica. I. França, Marcel Giovanni Costa. II. Universidade Federal de Minas Gerais. Instituto de Ciências Biológicas. III. Título.

CDU: 581

Ficha catalográfica elaborada pela bibliotecária Fabiane C M Reis – CRB 6 – 2680

UNIVERSIDADE FEDERAL DE MINAS GERAIS

FOLHA DE APROVAÇÃO

DEFESA DE DISSERTAÇÃO

ARTHUR DE BARROS RATES

Data: 28/01/2022 Entrada: 2019/2 Mat.: 2019724795 **CPF:** 09685953678

Título da dissertação aprovada: **"Aluminium and silicon induced changes in root cell wall composition and structure of *Zea mays* L."**

Comissão Examinadora

Dr. Marcel Giovanni Costa França (Universidade Federal de Minas Gerais)

Dra. Claudia Teixeira Guimarães (EMBRAPA)

Dr. Joni Esrom Lima (Universidade Federal de Minas Gerais)

Assinaturas dos membros da comissão

Documento assinado eletronicamente por **Claudia Teixeira Guimarães**, **Usuário Externo**, em 28/01/2022, às 11:43, conforme horário oficial de Brasília, com fundamento no art. 5º do Decreto nº 10.543, de 13 de novembro de 2020.

Documento assinado eletronicamente por **Joni Esrom Lima**, **Membro de comissão**, em 28/01/2022, às 11:48, conforme horário oficial de Brasília, com fundamento no art. 5º do Decreto nº 10.543, de 13 de novembro de 2020.

Documento assinado eletronicamente por **Marcel Giovanni Costa Franca**, **Professor do Magistério Superior**, em 29/01/2022, às 00:03, conforme horário oficial de Brasília, com fundamento no art. 5º do Decreto nº 10.543, de 13 de novembro de 2020.

Documento assinado eletronicamente por **Danilo Rafael Mesquita Neves**, **Coordenador(a) de curso de pós-graduação**, em 03/02/2022, às 13:56, conforme horário oficial de Brasília, com fundamento no art. 5º do Decreto nº 10.543, de 13 de novembro de 2020.

A autenticidade deste documento pode ser conferida no site https://sei.ufmg.br/sei/controlador_externo.php?acao=documento_conferir&id_orgao_acesso_externo=0, informando o código verificador **1188130** e o código CRC **46D9CCF3**.

Referência: Processo nº 23072.201005/2022-23 SEI nº 1188130

AGRADECIMENTOS

Ao Prof. Dr. Marcel França, por sua orientação, incentivo e apoio durante toda a preparação e execução dos trabalhos.

À Prof. Dra. Rosy Isaías, pelo apoio durante os experimentos de imunohistoquímica e por disponibilizar o laboratório de Anatomia Vegetal e os reagentes necessários para o projeto.

À Prof. Dra. Claudia Teixeira Guimarães, por disponibilizar as linhagens e plântulas de milho com enorme disposição e boa vontade, considerando as dificuldades impostas pela pandemia de COVID-19.

Ao Dr. Henrique de Castro Silva Junior do programa de pós-graduação em Química da Universidade Federal Fluminense (PGQ-UFF), por realizar os cálculos referentes às simulações moleculares deste trabalho e por ensinar-me como usar o programa Chemcraft, necessário para interpretar os dados gerados.

À Dra. Gracielle Bragança e ao técnico Wagner Afonso Rocha pela ajuda técnica com os protocolos de imunohistoquímica.

Aos colegas e amigos do laboratório de Fisiologia Vegetal, pelo apoio e companheirismo durante estes tempos difíceis de pandemia.

À Coordenação de Aperfeiçoamento de Pessoal do Ensino Superior (CAPES), pelo apoio financeiro disponibilizado por meio do Programa de Excelência Acadêmica (PROEX: Processo 88887.372427/2019-00).

RESUMO

O alumínio (Al) é o metal mais abundante da crosta terrestre e na sua forma catiônica é considerado tóxico para a maioria das espécies vegetais, provocando, na raiz, danos ao citoesqueleto, DNA, sistemas antioxidantes e metabolismo energético da célula. Como mecanismo de desintoxicação, a célula pode imobilizar Al em sua parede celular. Sabe-se que Al é capaz de ser retido em polissacarídeos pécticos e hemicelulósicos, como o homogalacturonano. A presença de Al na parede induz modificações em sua composição de forma a atenuar prejuízos aos processos de expansão e divisão celular. O silício (Si) é um elemento benéfico para as plantas e é um possível atenuador do estresse por Al por meio de mecanismos ainda não descritos. De forma a investigar as mudanças induzidas por Al na parede celular e avaliar os efeitos da adição de Si, duas linhagens de milho (*Zea mays* L.), uma resistente e outra sensível ao Al, foram cultivadas com e sem a presença de Al e Si. Em seguida, verificaram-se as mudanças na composição de polissacarídeos de parede pertencentes às classes de hemiceluloses e pectinas. Para complementar estes resultados, foram feitas análises computacionais utilizando o método DFT (Density Functional Theory) para simular possíveis estruturas químicas de compostos de polissacarídicos ligados a Al e Si. Foi encontrado que Al e Si induzem mudanças significativas na composição da parede celular de ambas as linhagens, sendo que ambos parecem atuar de forma sinergística, exacerbando os efeitos encontrados nos tratamentos com somente Al ou Si. Foram observadas mudanças visíveis na fluorescência de arabinano e xilano em ambas as linhagens, o que ainda não havia sido documentado na literatura. Também houve mudanças no conteúdo de homogalacturonano pouco metilesterificado na linhagem sensível e HG metilesterificado na linhagem resistente, o que corrobora resultados previamente descritos. As análises computacionais corroboram esses resultados, na medida em que se demonstrou a possibilidade de formação de complexos estáveis entre polímeros, Al e Si, os quais podem, inclusive, contribuir para a estabilidade da parede. Portanto, o trabalho demonstrou que as interações entre Al e Si *in muro* são complexas e que ocorrem mudanças na composição de todas as frações da parede, inclusive em polissacarídeos com funções ainda pouco conhecidas. São necessários mais estudos para melhor documentar os papeis fisiológicos desses elementos nas células, bem como para elucidar quais as funções específicas dos polissacarídeos de parede na resposta ao estresse por Al.

Palavras-chave: parede celular. Hemiceluloses. Pectinas. Alumínio. Silício. Imunohistoquímica. Density Functional Theory.

ABSTRACT

Aluminium (Al) is the most abundant metal on Earth's crust. In its cationic form, Al is toxic for most plant species, causing, in the roots, oxidative stress and damage to the cytoskeleton, DNA and energy metabolism. In order to promote detoxification, cells may immobilize Al in cell walls. It is known that Al can be adsorbed into pectic and hemicellulosic polysaccharides, such as homogalacturonan. The presence of Al in the cell wall induces changes in its structure to minimize its impact on cell expansion and division. Silicon (Si) is a beneficial element to plants, and may be a relevant Al stress attenuator, via yet-undescribed mechanisms. In order to investigate Al-induced changes in the cell wall and evaluate the effects of Si addition, two maize lines (*Zea mays* L.), one sensitive and another resistant to Al, were cultivated with or without the presence of Al and Si and analyzed for changes in the polymer composition of cell wall polysaccharides, via immunofluorescence assays. To complement these results, computational analyses were performed, using the DFT (Density Functional Theory) method, simulating possible chemical structures of complexes between polysaccharides, Al and Si. It was observed that Al and Si induce significant changes in the cell wall composition of both lines. Furthermore, both elements appear to act synergistically, with increased effects being observed in relation to either element alone. There were visible changes in xylan and arabinan fluorescence in both lines, a result previously undocumented in literature. Changes were also found in unmethylsterified homogalacturonan contents, in the sensitive line, and in highly methylsterified homogalacturonan in the resistant line, results supported by current published works. Computational analysis corroborates these results, indicating the possibility of the existence of stable complexes between polymers, Al and Si. These complexes may contribute to the stability of the cell wall. Therefore, this work demonstrated that the interactions between Al and Si *in muro* are complex and that there are significant changes in the composition of pectic and hemicellulosic fractions, even in polysaccharides with little-known functions. More studies are necessary to better document the physiological roles of these elements in plant cells, and to clarify the specific functions of cell wall polysaccharides in the response to Al stress.

Keywords: Cell Wall. Hemicelluloses. Pectins, Aluminium. Silicon. Immunohistochemistry. Density Functional Theory.

SUMÁRIO

1. INTRODUCTION

Aluminum (Al) toxicity is a widespread issue in tropical agriculture, and is responsible for significant crop losses (Kochian, 1995). Most plants exposed to soil Al exhibit symptoms such as stunted growth and root elongation inhibition, as well as damage on cellular and ultrastructural levels. Al is the most abundant metal on the Earth crust, and acid soils in tropical regions (ph <5,0) increase its availability to plants. Since land suitable for agriculture in tropical countries is usually scarce, agricultural practices in acid, Al-rich soils are getting increasingly common. Therefore, the impact of Al toxicity in crops is also becoming more prominent in these areas.

Al toxicity in plants mostly involves its trivalent cation form (Al3+), which is available in soils with pHs up to 5,0 (Macdonald and Martin, 1988). As the pH increases, other, less toxic forms of Al become available, as seen in figure 1. Therefore, Al toxicity is an agricultural problem mostly in acidic, highly weathered soils, such as *oxisols*, which are widespread in tropical regions (Brady & Weil, 2013).

Al uptake is mediated by the apical root region (Xia et al, 2010). Al is absorbed in the piliferous zone, and is transported via the apoplast in the root tissues. Several proteins may have a role in importing Al into the cell, such as the aquaporin (AQP) family (especially HmVALT and HmPALT1) and some transporters such as Nramps. After absorption, Al can be adsorbed to the cell wall or transported to the vacuole, cytoplasm or vascular tissues, where it is translocated to the shoot (Kochian et al, 2015; Huang et al, 2012; Negishi et al, 2013), via NIP1;2 transporters, while bound to malate (Wang et al, 2017), and other unidentified proteins. After entering the root, Al is likely sensed by cells through activation of a MAPK-dependent pathway (Arroyo-Seralta et al, 2005), although much of this mechanism still remains unknown.

Once inside the root tissue, Al can induce a range of physiological and biochemical stresses, both in the apoplast and symplast. After only a few minutes of Al exposure, root growth is inhibited, which results in stunted growth and cell death in the root tip (Porschneider 2002). In the cytoplasm, Al disrupts the cytoskeleton, interacting with actin and microtubules (Sivaguru et al, 2003), which may be directly related to the inhibition of cell elongation observed. Free Al ions also seem to interfere with cell signaling by altering cytosolic Ca^{2+} levels (Jones & Kochian 1995), which are essential second messengers in many signal transduction pathways in eukaryotes. Al also induces oxidative stress by increasing reactive oxygen species levels (Yamamoto et al 2001), as evidenced by the activation of radical scavenging enzymes such as

catalase, peroxidase and superoxide dismutase (Bhoomika et al, 2013; Sharma et al, 2007; for Al-induced oxidative stress and antioxidative pathways in animals, see Swain et al, 1997). High ROS levels may damage the plasma membrane and disrupt normal mitochondrial respiration (Huang et al, 2014). Therefore, Al toxicity is a complex and multifaceted process, which accounts for its high toxicity in most plants.

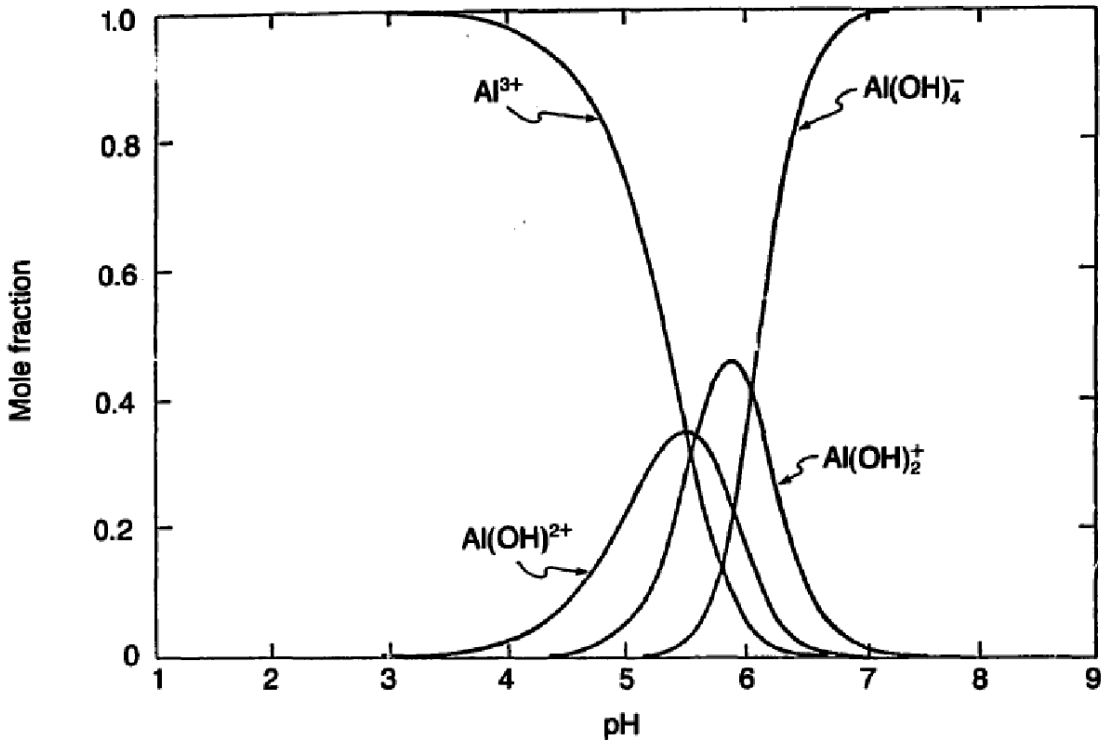

Figure 1 – proportion (=mole fraction) of available Al ions in relation to pH. From Macdonald and martin, 1988

Equally complex are the defense mechanisms employed by plants to resist Al toxicity. Al resistance can be divided in two categories (Kochian et al, 2015), exclusion and physiological tolerance. Al exclusion, which prevents Al from entering the root, is achieved by exudation of Al-chelating molecules in the rhizosphere. Organic acids are the most well characterized molecules involved in this process. Early experiments demonstrated a correlation between organic acid extrusion and Al resistance in some crops (Delhaize et al, 1993). This discovery led to a range of studies which characterized the role of organic acids in Al chelation. Malate and citrate, in their unprotonated form, easily bind Al and prevent its uptake by the root (Delhaize et al, 1993; Miyasaka et al, 1991). Malate is transported to the rhizosphere mainly by ALMT proteins (Al activated malate transporters, which are membrane ion channels belonging to the ARAE family of transporters (UniProt)). Al stress induces expression of ALMT proteins by activating Al responsive transcription factors such as STOP1 and its associated proteins (Fang et al, 2021), which are also implicated in the activation of other Al-resistance genes (Iuchi

et al, 2007). WRKY46, another Al-responsive transcription factor, is responsible for downregulating the expression of malate transporters. It is interesting to note that other members of the WRKY domain-containing family of transcription factors are also responsible for regulating other aspects of Al tolerance, especially cell wall modification. Citrate is transported by MATE (multidrug and toxic compound extrusion) proteins, which are organic acid/proton antiporters. Citrate transporter expression is regulated by an array of transcription factors, mainly ART1 (Al resistance transcription factor) and WRKY22 (Li et al, 2018) and ASR (Abscisic acid stress and ripening) proteins (Arenhart et al, 2013). Notably, ART1, as its name implies, is also involved in the regulation of 30 other genes related to Al tolerance (Xia et al, 2013). Acid exudation is a very important resistance mechanism in many crops, such as barley and sorghum (Magalhães et al, 2007; Delhaize et al, 2004), albeit other compounds, such as phenolics, and, possibly, UDP-glucose are also involved in Al chelation in some species (Tahara et al, 2014). A small, 53-residue cysteine-rich peptide bound to the plasma membrane is encoded by *CDT3* in rice and also shows Al-chelating capabalities (Xia et al, 2013), therefore possibly preventing Al from entering the cytosol. Al exclusion mechanism research has shown that many processes and classes of compounds are involved in Al chelation, which are integrated by transcription factors that regulate the expression of many genes at once.

Al tolerance, which is the capability of detoxifying Al that has entered the root, involves several distinct mechanisms. Cytoplasmic Al can be translocated into the vacuole, where it can be stored as a less toxic ion (Kochian et al, 2015), since the vacuole interior is more basic than the cytoplasm. This transport is mediated by aquaporin family members such as VALT1 (Negishi et al, 2012), at least in *Hydrangea macrophylla* sepal cells. It must be noted that, while it has recently been proven that aquaporin proteins are capable of transporting charged molecules (Byrt et al, 2017), it is likely that AQP translocate organic acid-Al molecules, which are uncharged (Wang et al, 2017). An ABC (ATP-binding cassette) transporter, ALS1, also actively transports Al into the vacuole in rice (Huang et al, 2012).

As mentioned, Al causes oxidative damage to cell components and activates anti-oxidant machinery to alleviate or avoid these stresses. The most common species that cause oxidative damage are superoxide anion (O_2^-), hydrogen peroxide (H_2O_2), hydroxyl radical (–OH), and singlet oxygen ($^1O_2$) (Munné-Bosch et al, 2001), while other, less common nitrogen radicals are also involved. These compounds also attack DNA molecules, causing mutations especially in guanine and adenine nucleotides (Shukla et al, 2009). Therefore, having an efficient

antioxidant system is essential to Al tolerance. In fact, Giannokoula et al (2010) showed that an Al-sensitive maize (*Zea mays*) inbred lineage lacked the upregulation of two antioxidant enzymes which conferred Al resistance to the tolerant lineage.

The primary cell wall (CW) is the other compartment that can bind or store Al and thus affect tolerance. Three classes of polysaccharides are responsible for most of the CW's load-bearing capacity: cellulose, hemicelluloses and pectins. Traditionally, the CW is viewed as a composite of cellulose microfibers, interconnected by hemicelluloses or cross-linking glycans, all embedded in a gel-like matrix of pectins. Each component will be shortly characterized to provide a better understanding of the role of the CW in Al binding.

Cellulose is the most abundant polysaccharide of the CW. It is a homopolymer of glucose (Glc) units connected by β-1,4 glycosidic linkages. This means that the link between two Glc residues was formed between carbon 1 (the reducing or anomeric carbon) of β-glucose (meaning that the –OH group of carbon 1 was in its axial, and not equatorial, position) and carbon 4 (nonreducing) of the following residue (Berg et al, 2019). These β-1,4 bonds favor the formation of a rigid and planar structure, unlike the α-1,4 bonds of amylose, starch, glycogen and of some pectins, which create more flexible and compact polymers (Berg et al, 2019). Cellulose synthase complexes are responsible for synthesizing cellulose at the cell wall site, forming transverse fibers which are dependent on microtubule orientation (Paredez et al, 2006). While cellulose is the most abundant polymer in the CW, it has no known Al-binding capabilities, although cellulose synthase is inhibited by Al in roots (Teraoka et al, 2002).

Hemicelluloses, also called cross-linking glycans, are a group of substituted polymers primarily based on a β-1,3 or β-1,4 xylan (xylose) or cellulose backbone. Attached to the backbone are sugars including arabinose and glucuronic acid. The most abundant hemicellulose in noncommelinid eudicots is xyloglucan (XG), which is composed of a backbone consisting of Glc and Xyl residues with Xyl attached at C6. Species belonging to the order Poales (grasses and cereals) have another type of hemicellulose, which is the mixed-linkage glucan (Ebringerová, 2006), consisting of an unbranched polymer of three of four β-1,4 Glc chains linked by β-1,3 Glc residues. A common feature of all hemicelluloses is that they bind strongly to cellulose, therefore helping spread physical forces impacting the CW (Ebringerová, 2006).

Pectins, which form a gel-like matrix which interacts with all other components of the CW, are classified into four polymers. The simplest one is homogalacturonan (HG), is a α-1,4 linked galacturonic acid (GalA) homopolysaccharide (Buchanan et al, 2017). The structure of

xylogalacturonan (XG) is the same of HG but with added Xyl residues at O3. Rhamnogalacturonan II (RG-2), despite its name, has a basic backbone of HG with several attached side chains, which consist of an incredible variety of sugars. In fact, RG-2 is the most complex plant polysaccharide known, surpassing the diversity of lignin (Buchanan et al, 2017). Rhamnogalacturonan I (RG-1) has a backbone of alternating GalA and rhamnose (Rha) linked by α-1,2 and α-1,4 bonds, as well as linear and nonlinear side chains of oligosaccharides such as arabinan and galactan attached at O4. The alternating α-1,2 and α-1,4 bonds favor a rod-like conformation which sets it apart from other pectins. For a simplified guide to the structures of some hemicelluloses and pectins, see **figure 2.**

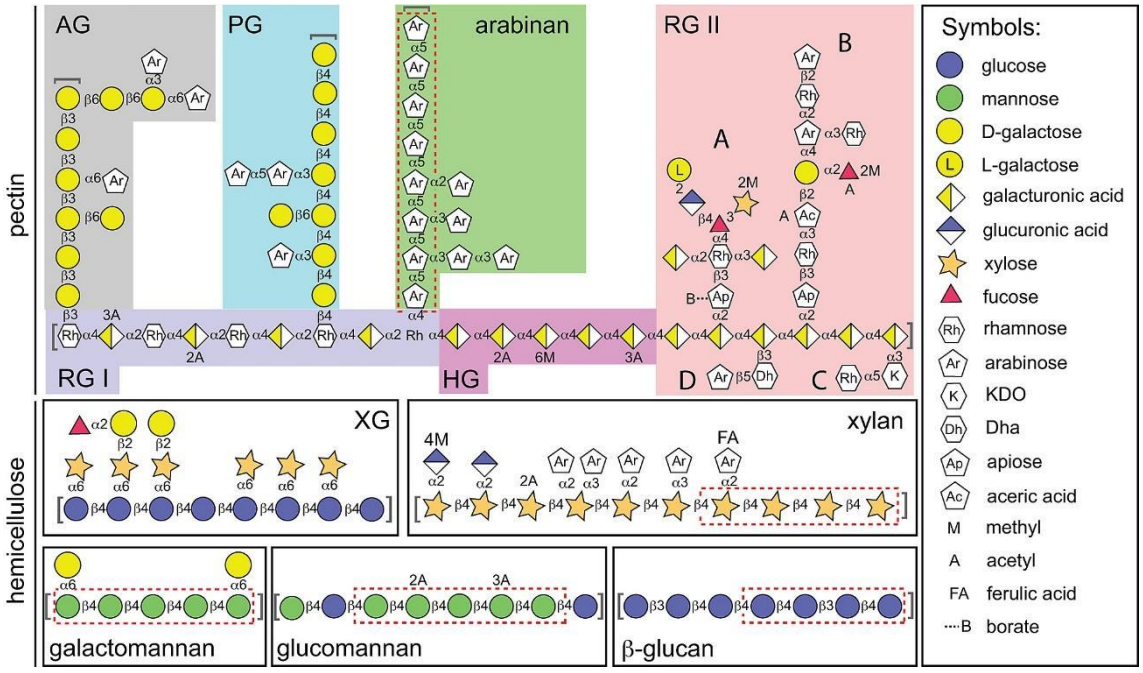

Figure 2 – simplified representations of some pectin and hemicellulose polysaccharides. The structure of RG-2 symbolizes only some sugars that decorate its backbone. From Martens et al, 2011.

It is important to note that the ratio of each component varies between phylogenetic groups, with two main types of architecture being predominant: type I cell walls occur in non-Commelinid species, and type II walls occur exclusively in members of the Poales (Albersheim et al, 2011).

The synthesis of these CW components is a complex and ongoing field in plant biology and glycobiology. β-linked glycans are synthesized by Cellulose synthase-like (CSL) family glycosyltransferases (GTs) in the Golgi apparatus lumen, and then transported by vesicle secretion to the plasma membrane surface. These enzymes use activated sugars, that is, a nucleotide-bound monosaccharide, to transfer a monosaccharide to a growing chain (Kim & Brandizzi, 2016). Most sugars are linked to uridine diphosphate (UDP), such as UDP-Glc, but

other residues can be attached to thymidine, adenine, guanine, or, more rarely, cytidine diphosphate (Albersheim et al, 2011) Plants contain dozens of *CSL* genes, which are divided into nine subfamilies labeled from A-H (Keegstra & Walton, 2006). Most of these enzymes have unknown function, but the general function of each gene subfamily has been identified (Kim & Brandizzi, 2016). For example, *CSLF* encodes proteins responsible for mixed-linkage glycans of grasses (Burton et al, 2006). Most xylose-backbone polymers (xylans), which make up the bulk of primary and secondary cell wall dry weight along with cellulose, are synthesized using UDP-glucose as an initial substrate. UDP-Glc, which is a 6-carbon sugar, is converted into UDP-Xylose, a 5-carbon sugar, by UDP-Xyl synthase, in the cytosol or Golgi lumen (Rennie & Scheller, 2014). UDP-Xyl is then added onto the non-reducing end of the xylan chain by a protein complex likely involving several *IRX*-encoded (*Irregular Xylem*) units. Other sugars and carbon molecules can be added onto this backbone, including arabinose, acetate, glucuronic acid and ferulic acid. The type and frequency of these decorations varies between species and also tissues. For example, grass xylans are initially synthesized with several acetylated or feruloylated sugars, and are progressively stripped of these features as the tissue ages. These modifications, therefore, implicate that there are mechanisms that modify hemicellulose composition and properties in a time-dependent manner. Parallel to this, hemicelluloses are also modified according to biotic or abiotic stress (Rennie & Scheller, 2014), which adds yet another layer of complexity to an already vast network of enzymes and genes that work to maintain or modify cell wall properties according to tissue, age or environmental cues.

Meanwhile, pectins are synthesized by α-linking GTs. Since plants have over 600 identified GTs, and considering that most of these proteins are found in very low concentrations (Albersheim et al, 2011), discovering the process of pectin synthesis has been slow and difficult. HG is synthesized by glucuronosyltransferases (GAUT), with at least two (GAUT1 and GAUT7, which likely associate *in vivo*) being responsible for vegetative cell wall synthesis (Atmodjo et al, 2011). Many other, putative GAUT proteins are also presumed to synthesize pectins (Caffal 2008). The identification of GTs involved in the synthesis of oligosaccharides that comprise the side chain of hemicelluloses and pectins is constantly increasing, and new proteins are registered and classified in the Carbohydrate-Active enZymes Database (CAZy), which currently has information on over one hundred GT families (Lombard et al, 2014).

The cell wall is a dynamic structure which responds to intra and extracellular signals (Voxeur and Höfte, 2016). Therefore, it is constantly being remodeled to accommodate cell growth and

respond to biotic and abiotic stresses. For example, the CW must be modified to allow or arrest cell elongation. Several enzymes are implicated in remodeling and changing the physical and chemical properties of the CW, and play a very important role in Al resistance in most plants. After secretion, polysaccharides may be cleaved at an internal bond, which is the function of endohydrolases (Osato et al, 2006). Recently, hydrolases that specifically cleave xyloglucan chains were proven to greatly affect the CW Al binding capabilities of *Arabidopsis*, with at least two (XTH17 and XTH31) being directly involved in modulating Al sensitivity (Zheng et al 2012; 2014). Zheng et al (2012) demonstrated that, at least in *Arabidopsis*, decreasing xyloglucan content significantly decreased Al bound to the CW as well, therefore indicating that the activity of XTH enzymes may predispose plants to accumulate Al in the CW and amplify its toxicity. Therefore, investigating the role of CW components in Al toxicity not only requires evaluating the role of each polysaccharides, but also analyzing the modifications that happen after secretion and deposition.

Whether hemicelluloses or pectins are the main site of CW Al accumulation is still a matter of much debate, as some authors (Zheng et al, 2014; Zhu et al, 2012) finding that hemicelluloses bind most Al, and others reaffirming the more traditional view that pectins are the main site of Al accumulation (Yang et al, 2008). For the latter, it is generally accepted that HG plays the most prominent role in CW elongation and Al binding (Albersheim et al, 2011). Before delving into the possible factors that affect CW properties, it is important to clarify the meaning of the parameters used to describe them. Wall loosening or stiffening refers, in most works, to the ability of the wall to stretch or resist stretching. This can be measured by rheological creep experiments, in which a small weight (tensile force) is attached to the tissue in question, and monitoring the change in length (for a protocol, see Durachko et al, 2017). Wall loosening allows an increase in wall length, driven by the turgor pressure of the protoplast. In turn, the increase in length allows for cellular expansion.

HG is secreted in a highly methylsterified form, that is, with a methyl (-CH3) attached to the carboxyl group of GalA (Kim et al, 2016). Since in cellular conditions the carboxyl group is deprotonated (and therefore negatively charged), adding a methyl group to it significantly modifies the polymer charge and chemical properties. HG can cross-link with other HG chains via a Ca^{2+} bridge that binds two adjacent GalA residues (Yang et al, 2008), and this helps stiffen the CW. These dimers form characteristic “eggbox”-like structures. However, these cross-links can only form between charged, unsterified residues. Pectin methylesterases (PME) are responsible for oxidative hydration of the methyl group from the sugars, releasing methanol.

Up until recently, the predominant view of PME function is that they allow stiffening of the cell wall by producing polygalacturonate chains capable of forming the aforementioned rigid eggbox Ca^{2+}-dimers. However, more recent studies challenge this hypothesis. For example, Wang, Wilson and Cosgrove (2020) demonstrated that PME activity softens the CW while maintaining its elasticity. This means that the wall becomes more plastic (prone to physical deformation) but not looser, as measured by cell wall creep. Therefore, it is important to note that wall loosening may happen independently of other rheological properties, and PME activity alone is not sufficient to explain the modification of CW properties seen during cell expansion. Other factors that affect CW properties include Ca^{2+} availability (in the experiments conducted by Wang, Wilson and Cosgrove (2020), the CW displayed opposite changes in plasticity depending on the availability of Ca^{2+}), and the activity of other enzymes acting downstream of PME, such as polygalacturonases. Unsterified HG is the substrate for polygalacturonases which degrade pectin (Moustacas et al, 1991). Thus, polygalacturonase activity may be responsible for the loosening previously attributed to PME (Hofte et al, 2012).

On the other hand, unsterified HG also binds Al with high affinity. In one experiment, Yang et al (2008) showed that an Al-sensitive rice lineage had greater levels of unsterified HG than a resistant lineage. In another study, it was shown that boron (B) decreases Al toxicity in rice by reducing its binding to the CW, and also by repressing pectin synthesis and PME activity (Yan et al, 2021). Therefore, pectin is also a major site responsible for Al sensitivity. However, it is still unclear how it affects CW properties, and the precise locations it binds on the polymer structure itself.

Over the years, several treatments have been shown to alleviate Al toxicity in plants, including increasing CO2 concentration (Zhu et a, 2017) and addition of several compounds such as hydrogen sulfide, boron and silicon (Si) (Zhu et al, 2018; Li et al, 2017; Yan et al, 2018; Pontigo et al, 2017). Of these, Si is notable because it is the second most abundant element on Earth's crust (*CRC Handbook of Chemistry and Physics, 2017)*, closely followed by Al. Hence, Si is one of the main constituents of the soil solution in contact with plant roots and is absorbed in the form of silicic acid (H4SiO4, which is in equilibrium in aqueous solution with its anhydride Si(OH)4, named orthosilicic acid). All the same, it is not an essential element to most species, and is considered by most authors to be beneficial to growth (Taiz & Zeiger, 2017) ever since the beginning of the twentieth century (Sreenivasan, 1934). This is in spite of Si having similar concentrations as essential macronutrients (up to 1mM, comparable to sulfur, potassium, calcium and magnesium (Epstein, 1990). Therefore, Epstein (1994) considered Si to be

somewhat of a biological anomaly, due to its abundance and concomitant scarcity of biological functions. In recent years, interest over the biological functions of Si in plants has rapidly grown, given its ever-increasing portfolio of beneficial effects on agriculturally relevant parameters such as biomass accumulation.

A group of aquaporin/NIP (Nodulin 26-like Intrinsic) proteins has been found to be responsible for silicic acid influx into cells (namely, Lsi1 and Lsi6 (Deshmukh & Bélanger, 2016)). These proteins, which are assembled as tetramers in the plasma membrane, have a unique G-S-G-R amino acid selectivity filter, and are able to passively transport, in general, water and other small uncharged molecules. On the other hand, another group of anion transporters (Lsi2 and Lsi3) promotes its active efflux to the apoplast (Ma et al, 2007) and to vascular tissue (Ma & Yamaji, 2015). These active transporters have, unlike the influx transporters, a single polypeptide chain consisting of up to 12 transmembrane domains, which are responsible for the energy-dependent efflux of silicic acid. However, these transporters are present mostly on the root exo and endodermis, and movement through aerial tissue parenchyma is thought to be apoplastic (Deshmukh & Bélanger, 2016). In tandem, Lsi1/6 and Lsi2/3 work to form a favorable gradient for Si influx from the soil solution into the root. In addition, Lsi6 appears to promote Si xylem unloading into the leaf parenchyma. Interestingly, Lsi2 is also responsible for arsenite (AsO3) influx into rice roots (Ma et al 2008) and therefore are also subject to intensive research in the field of arsenic toxicity, which is a problem for agriculture especially in Asian countries (Meharg & Raman, 2003; Abedin et al, 2002).

After the publication of Epstein's seminal works in the 80s and early 90s, the known functions of Si in plants have greatly increased. Si was first found to increase tissue strength and resistance to herbivory (Hartley & DeGabriel, 2016; Frew, Weston & Gurr, 2019; Lin et al, 2019). Currently, several studies demonstrate that Si is beneficial in alleviating a wide range of abiotic stresses, including salt, drought, cadmium and Al stress. Si also has beneficial effects beyond stress alleviation, positively modulating nutrient acquisition by the roots (Barreto et al, 2017). A small summary of the effects of Si in macronutrient metabolism will be provided to better illustrate its important effects on plant growth. Si has been shown to improve all aspects of N metabolism in plants (acquisition, assimilation and remobilization), even in suboptimal supply conditions (Esteban et al, 2016; Mabagala et al, 2020; Pati et al, 2016; Cuong et al, 2017). Indeed, Si upregulates the expression of many genes involved in N metabolism, especially those related to uptake (*NTR* and *ATR* genes) and assimilation (i.e. GS-GOGAT cycle genes - *GS2*, *Fd-GOGAT*, *NADH-GOGAT2*, *GDH2* and *NR1*). Enhanced growth of Si-fed plants exposed to

high N concentration is also often attributed to increased photosynthetic efficiency, antioxidant capacity and improved water status (Barreto et al., 2017). The effects of Si on phosphorus (P) metabolism have also been extensively studied. It has been shown that it modulates P availability in opposite scenarios, that is, in deficiency and excess P conditions, possibly by differentially regulating PHT transporters according to its availability (Kostic et al, 2017; Owino-Gerroh & Gascho, 2005). Si also has direct effects on potassium use by plants in K-limited conditions, but the underlying mechanisms are not well understood. Some studies show that Si increases K transport directly or indirectly by modulating H+-ATPase activity or K transporter activity (Liang et al, 2003; Yan et al, 2021), while others indicate no change in internal K levels but exhibit improvement of K-related parameters such as photosynthesis and water conductance in xylem vessels (Chen et al, 2016). Finally, Si improves calcium (Ca) uptake under most conditions, but studies show conflicting results depending on growth parameters and stress types (Greger et al, 2018; Cooke & Leishman, 2016).

Al stress is alleviated by the addition of Si through several proposed mechanisms, both in the plant or in the soil solution. Si increases the pH of the soil solution, thus limiting the availability of toxic Al cations for root uptake (Li et al, 1996). In addition, Si may also react with Al species, forming hydroxyaluminosilicates that are inert in the soil or apoplast (Exley & Birchall, 1992). Some studies suggest that Si modulates Al transporter expression or activity, thus limiting Al intake (Pontigo et al, 2017; However, there is a remarkable lack of experimental evidence concerning the interactions of the two elements *in planta*, with most studies focusing on each element separately.

While Si is a beneficial element to most plants, many authors consider it essential for Poaceae species (Epstein ,2009), with several being Si hyperaccumulators, such as rice (Savant et al, 1997), which accumulates up to 10% of its shoot dry weight in Si. In the CW, Si may bind primarily to pectins (He et al, 2015) through direct organosilicon (C-O-Si) linkages, rather than being deposited as amorphous silica (He et al, 2013), and therefore may help structure the CW.

Along with other grass species, maize (*Zea mays*) is one of the most extensively cultivated food crops in the world, being a staple in many cultures of Latin America, Africa and Asia. Maize alone is responsible for approximately 15% of protein consumed annually (Pandey et al, 2004). Maize was domesticated from wild Mexican teosinte (*Zea mays* ssp. *parviglumis*) (Doebley, 2004), which had undesirable traits such as a hard, heavily lignified structure covering the kernels that prevents herbivory and destruction of the seed in animal digestive tracts (Wang et al, 2015). The expansion of maize agriculture in developing countries has led to the arousal of

challenges regarding the adaptation of varieties to tropical, acid and nutrient-poor soils. In Brazil, several lineages have been developed both by private companies and by the Empresa Brasileira de Pesquisa Agropecuária (Embrapa), a publicly-funded company for the development of solutions for Brazilian agriculture. Indeed, Embrapa has developed several maize varieties in use today, some of which sensitive and others resistant to Al stress. Based on previous data produced by Embrapa and other authors (Maron et a, 2010), we used an Al-resistant and an Al-sensitive lineage of Z. mays to investigate the differences in the cell wall response to Al toxicity in these lineages, and the effect of Si addition to these responses.

To further clarify the relationship between Al and Si *in planta*, we employed computational analysis based on quantum physics to determine the probable structures of Al/Si/polysaccharide complexes. The technique, called Density Functional Theory (DFT), is a modelling method which uses electron density to investigate the structure of atoms and molecules, producing optimal energy surfaces (i.e. with the minimum energy possible) that can indicate the viability of the structure or its stability when compared to other structures (i.e. with lower total potential energy than others). While the mathematical theory behind this method is beyond the scope of this work, DFT is garnering significant attention due to its many applications in the life sciences: several studies have used it in the field of medicine to investigate the interactions between anti-cancer drugs and their organic carriers (Shaki et al, 2019), antivirals (Li Feng et al, 2013), plant-derived radical scavengers (Nakanishi et al, 2020; Vo et al, 2018) and many others. Additionally, DFT has been used to investigate the chemical properties of several plant compounds, mostly cyclic molecules such as phenylpropanoid-derived molecules and flavonoids (Rammohan et al, 2020; Rahman et al, 2015).

2. OBJECTIVE

We aimed at comparing the compositional changes in root cell wall hemicelluloses and pectins of two lineages of *Zea mays* L., one sensitive and another resistant to Al, treated with combinations of aluminum (Al) and silicon (Si), two non-essential elements for plants with contrasting physiological effects.

2.1 SPECIFIC OBJECTIVES

- Gather, organize and classify available evidence for primary cell wall biosynthetic enzymes by reviewing published articles and systematic reviews;

- Document the changes in pectin polysaccharides arabinan, unsterified homogalacturonan and methylsterified homogalacturonan, and hemicellulosic xylan in *Zea mays* roots treated with Al and/or Si using fluorescent monoclonal antibody probes.
- Compare the cell wall responses to Al and Si treatments in roots of an Al-tolerant lineage, Cateto Al237, and an Al-sensitive line, L53.
- Determine if the observed cell wall responses occur shortly after exposure (<24h) or over longer periods (<48h).
- Evaluate possible Al and Si binding sites in polysaccharide monomers using density functional theory (DFT) computational analysis.

3. METHODS

3.1 REVIEW OF CELL WALL CARBOHYDRATES, POLYMERS AND GLYCOSYLTRANSFERASES INVOLVED IN PRIMARY WALL SYNTHESIS

A review of available data was conducted using two primary databases, PubMed (https://pubmed.ncbi.nlm.nih.gov) and Periódicos CAPES (https://www-periodicos-capes-gov-br.ezl.periodicos.capes.gov.br/). A systematic search was performed using the boolean operators 'glycosyltransferase' AND 'cell wall' AND [c.w.c], where c.w.c is the cell wall component in question, such as 'rhamnogalacturonan I'. Then, another search was performed using boolean operators 'cell wall' AND [c.w.c] AND 'function' in order to assess available evidence for the function of each polymer. Results concerning bacterial cell wall enzymes were excluded from both searches. When available, the same references were used to reunite data concerning the composition of each monomer, including general conformational isomerism (f or p forms), enantiomerism (D or L configuration), type (α or β) and position of glycosydic linkages. To organize results, a table was produced with seven columns, which include the following information:

1. 'NAME': the name of the cell wall polysaccharide and type, when applicable.
2. 'CW FRACTION': which fraction (i.e hemicellulosic or pectic) the polymer is more frequently encountered.
3. 'MONOSACCHARIDE COMPOSITION': which carbohydrates are present in the structure of the polysaccharide. α or β refer to the configuration of the anomeric carbon and the consequent configuration of the glycosydic bond; D or L refer to the light-polarizing enantiomeric configuration (Levorotatory or dextrorotatory), based on the configuration of the carbon furthest from the ketone or aldehyde group; f or p refer to

the configuration of all carbons, which may resemble a pyran ring (“hexagonal shape” or a furan ring (“pentagonal shape”).

4. ‘TYPES OF LINKAGES’: position of the reducing carbon: position of the reduced carbon.
5. ‘FUNCTION’: general described functions of the polysaccharide in the cell wall.
6. ‘BIOSYNTHETIC ENZYMES’: which glycosyltransferases transfer an activated sugar donor to the growing polysaccharide chain. In parenthesis are the families of the enzymes according to the classification system used by the CAZy database. In brackets are the specific transfer reactions catalyzes by the enzyme.
7. ‘REFERENCES’: references directly used in the review process.

3.2 PLANT GROWTH CONDITIONS

All plants used in this work were cultivated at Embrapa Milho e Sorgo (Sete Lagoas, Minas Gerais, Brazil). Seeds from the Cateto and L53 lineages were hygienized using 0,4% sodium hypochlorite and placed in wet filter paper. The paper was wrapped around the seeds in order to evenly distribute humidity and allow for the development of linear roots. After germination, Seedlings were transferred to polyethylene cups placed into containers filled with 8.5 l of nutrient solution at pH 4.0, under continuous aeration, and acclimatized in full nutrient solution for 24 h. In experimental groups, Al treatments were imposed by replacing the nutrient solution with nutrient solution of identical composition but with or without {222} μM Al^{3+} activity supplied as $KAl(SO_4)_2$. Si-treated plants were also exposed to the same nutrient solution but with 5 mM SiO_2 (silicon dioxide) and Na_2O (sodium oxide solution; Diatom Mining) also added. The pH was adjusted to 4,0 for every treatment group. Each group contained 7 seedlings. After the duration of the experiment (24 or 48h), seedlings were removed from the nutrient solution, washed with deionized water, hand-sectioned approximately 1 cm from the apex and placed in Karnovsky fixative (2% paraformaldehyde, 2.5% glutaraldehyde in phosphate buffer solution (PBS) 0,05 mol/L at pH 7,4) until further processing.

3.3 IMMUNOFLUORESCENCE ASSAYS

Three roots were randomly selected from the seven previously fixated. Roots were subsequently dehydrated in an ethanol series starting at 10% ethanol up to 95% ethanol with half-hour changes. Afterwards, they were placed in eppendorfs containing a pre-infiltration solution for 24h and then in an infiltration solution for 24h at 4°C. After this period, roots were placed in chilled, flexible 6x8mm molds filled with a Leica™ Historesin and 0,06% hardener solution.

The histomold was then wrapped in PVC film and placed in freezer conditions (-10°C) for 24h, then left at room temperature for 2h to allow hardening.

6um-thick cross sections, containing three roots each, were cut from the resulting resin blocks using a Jung™ Biocut microtome and placed on glass slides, which were then taken to antibody incubation.

Each slide, containing 3 sections/replicates, was incubated for 0.5h in 3% milk powder/PBS solution and then in a 10uL 20% PBS solution containing PlantProbes LM6, 10, 19 or 20 monoclonal antibodies for 2h. Milk powder is an effective protein blocking agent as it contains bovine serum albumin (Baldo et al, 1986). The targets for each probe can be found in table 1. Each section was then washed with PBS and incubated in the dark for 2h with 10uL 1% anti-rat secondary antibody conjugated with fluorescein (FiTC; Thermo-Fisher Scientific) solution. The slides were washed with PBS, mounted in 50% glycerin and immediately taken to observation using a Leica™ Laser scanning confocal microscope. Pictures were captured at 10, 20 or 40x magnification using Leica Application Suite (LAS) software, and basal fluorescence was eliminated by adjusting exposure according to a blank slide (root cross-sections treated only with PBS/milk powder solution).

Table 1 – Rat monoclonal antibodies (MAbc) used in immunofluorescence procedures. All probes were acquired from and produced by the Paul Knox Cell Wall lab at the University of Leeds (UK). Me-HG: methyl-esterified homogalacturonan; LM: Leeds Monoclonal antibody.

MAbc	**Target**	**Reference**
LM6	(1□5)-⟨-L-arabinan	Jones et al. (1997)
LM10	(1□4)-®-D-xylan	McCartney et al. (2005)
LM19	low Me-HG / no ester	Verhertbruggen et al. (2009)
LM20	high Me-HG	Verhertbruggen et al. (2009)

3.4 POLYSACCHARIDE AND AL/SI INTERACTION ANALYSIS BY DENSITY FUNCTIONAL THEORY (DFT)

Density Functional Theory (DFT) is a method based on quantum physics used to describe molecular structures based on electronic density (Morgan & Custodio, 1995), when analytical characterization is insufficient or impossible to obtain. Electronic density, p(r), is the underlying tridimensional function which describes the distribution of charges on a given molecule.

In order to obtain representative structures of cell wall polysaccharides, a formalism from the theory was used and implemented in the SIESTA computer program (Soler et al, 2012). This program is capable of calculating the structure of very large molecules and polymers using first-principle electronic structure methods, and has therefore been adopted by several fields in the applied and life sciences, including biology, engineering, medicine and geosciences (Garcia et al, 2020). Initially, representative structures of hemicelluloses were optimized based on their monomer composition. Then two different structures were generated, one including only two monomers and Al/Si, and another including the interactions between Al, Si and four independent monosaccharides. The combination of Al/Si was shown in our monoclonal antibody assays to yield related or synergistic results. To calculate the structures, DLPNO-CCSD(T)/cc-pVTZ theory level calculations were used, which yield very robust results comparable to or better than experimental data. Final structural features were based on potential energy surface linked to electronic distribution on each atom. All structures were then optimized by using composite method PBEh-3C and the absorbance and vibrational spectra were calculated using D3/Def2-TZVP theory level.

4. RESULTS

4.1 CELL WALL CARBOHYDRATES

The synthesis of the CW is a complex, polygenic process (Albersheim et al, 2011) which is constantly being revised and updated. In order to better establish the genetic background that underlies the cell response to Si and Al, we performed a systematic search on scientific databases to summarize genes and enzymes directly involved in CW synthesis, as well as the known functions and composition of each polysaccharide. Table 1 highlights the great diversity of proteins involved in CW synthesis. Notably, there is very little information available on arabinogalactan proteins and on RG-II synthesis and function.

Table 2 - summary of plant primary cell wall polysaccharide composition, function and biosynthetic enzymes according to available literature. Biosynthesis enzymes are presented as follows: NAME OF PROTEIN (Glycosyltransferase family; e.g. GTF31, according to the CAZy database) (Types of glycosidic bond formation catalyzed). Additional information regarding protein function is also reported when available.

NAME	CW FRACTION	MONOSACCHARIDE COMPOSITION	TYPES OF LINKAGES	FUNCTIONS	BIOSYNTHETIC ENZYMES	REFERENCES
Arabinan ("type 2" – present in arabinogalactan proteins)	Extracellular AGPs	α-L-arabinose f	1:5	-		Albersheim et al (2011)

Arabinogalactan (type 2 – present in arabinogalactan proteins)	Extracellular AGPs	α-L-arabinose f β –D-galactose p 4-Me-D-glucuronic p acid L-fucose f D-glucuronic p acid	1:3 (Gal-Gal) 1:6 (Gal-Ara) 1:6 (Gal-Gal) 1:5 (Ara-Ara) 3:5 (Ara-4-Me-D-GlcpA) 1:4 (GlcpA-GlcpA)	Controls cell shape by influencing cortical microtubule organization	GALT2:6 (GALACTOSYLTRANSFERASES) (GTF31) (1:3 Gal-Gal) GALT29A, GALT31A (GTF29; 31) (1:6 Gal-Gal) HPGT1:3 (HYDROXYPROLINE O-GALACTOSYLTRANSFERASE) (GTF31) (initial Gal-Hyp) RAY1 (REDUCED ARABINOSE YARIV 1) (GTF77) (1:6 Gal-Ara)	Yoshimi et al (2020) Ogawa-Ohnishi et al (2015) Gille et al (2013) Makarova et al (2016)

Arabinoxylan/glucuronoarabinoxylan	HC (mostly grasses)	α-L-arabinan f β-D-xylose f Ferulic acid *p*-coumaric acid α-D-glucuronic acid 4-*O*-Me-glucuronic acid 4-O-methyl glucuronic acid D-galactose p	1:4 (main xylan chain) 1:2 (Ara: Ara, Ara – GlcA and Ara-MeGlcA) 1:3 (Xyl-Ara)	Ferulic acid cross-links regulates cell wall extension and is affected by environmental cues	IRX9/10/14 (IRREGULAR XYLEM) extends xylan chain (GTF47) XAT (XYLAN ARABINOFURANOSYLTRANSFERASE) (GTF61) (1:3 Xyl-Ara) XAX (ARABINOXYLAN ARABINOSYLTRANSFERASE) (GTF61) (1:2 Ara-Ara) GUX1/2/3 (XYLAN GLUCURONOSYLTRANSFERASE) (GT8) FRA8 (FRAGILE FIBER 8) (1:4 MeGlcA-Xyl)	Grabber et al (1995) Wakabayashi (2015) Mortimer et al (2010) Anders et al (2012) Lee et al (2012) Zhong et al (2005)

Xyloglucan	HC (mostly eudicots)	β –D-glucose p α-D-xylose f β-D-galactose α-fucose	1:4 Glc-Glc (main glucan) 1:6 Xyl-Glc 1:5 Gal-Xyl 1:2 Fuc-Gal	Main component of eudicot HC Tethers cellulose microfibrils Wall tightening	MUR3 (galactosyltransferase activity) XT1, XT2 (XYLOSYLTRANSFERASE) (GTF34) (1:6 Xyl-Glc) FUT1 (FUCOSYLTRANSFERASE 1)	Takahisa & Rumi (2011) Madison et al (2003) Cavalier et al (2006) Perrin et al (1999)
Xylan	HC	β-D-xylose f Glucuronic acid (mostly dicots)	1:4 Xyl-Xyl	Vessel wall; xylem fiber formation Secondary wall component; Complexes with lignin units.	FRA8 (FRAGILE FIBER 8) (1:4 MeGlcA-Xyl) MUCI21 (MUCILAGE RELATED) essential for synthesis IRX9/10/14 (IRREGULAR XYLEM) (GTF47) (1:4 Xyl-Xyl)	Zhong et al (2005) Rennie & Scheller (2014) Voiniciuc et al (2015a)

Mixed-linkage glucan	HC (in grasses)	β-D-glucose	1:3;1:4 Glc-Glc	Accumulates in expanding tissues; in xylem fibers and vessels	CslF6 (Cellulose synthase-like F6)	Vega-Sánchez et al (2012)
Mannan	HC	β-D-mannose	1:4 Man-Man	Storage polysaccharide	CslD1/2/3/5 (Cellulose synthase-like D1/3/5) CslA12 (in endosperm)	Verhertbruggen et al (2011; 2021)
Galactomannan	HC	β-D-mannose α-D-galactose	1:4 Man-Man 1:6 Man-Gal	Storage polysaccharide in legume seeds	CslD1/3/5 (Cellulose synthase-like D1/3/5) MAGT1/MUCILAGE-RELATED10 (MUCI10) [1:6 Man-Gal]	Verhertbruggen et al (2011) Schröder et al (2009) Voiniciuc et al (2015)
Glucomannan	HC	β-D-mannose β-D-glucose	1:4 Man-Man 1:4 Man-Glc	Storage polysaccharide in monocot seeds, and in bulbs and tubers Structural support in woody tissues Embryogenesis	CslA2/3/7/9 (Cellulose synthase-like A2/3/7/9) [1:4 Man-Glc]	Goubet et al (2009) Schröder et al (2009)
Galactoglucomannan	HC	β-D-mannose β-D-glucose α-D-galactose	1:4 Man-Man 1:4 Man-Glc 1:6 Man-Gal	Storage polysaccharide Structural support in some species	MAGT1/MUCILAGE-RELATED10 (MUCI10)	Schröder et al (2009) Gille et al (2011) Voiniciuc et al (2015)

Xylogalacturonan	P	α-D-galacturonic acid β-D-xylose f	1:4 (main galacturonan) 1:3 (Xyl-GalA or Xyl-Xyl)	General pectin structure Formation of Ca^{2+} bridges Pathogen resistance	XGD1 (XYLOGALACTURONAN DEFICIENT1) (GTF47) [1:3 Xyl-GalA]	Jensen et al (2008)
Homogalacturonan	P	α -D-galacturonic acid	1:4 GalA-GalA	Main pectic component Ca^{2+} bridge formation Controls cell wall extensibility	GAUT1/7 (GALACTURONOSYLTRANSFERASE); (GTF8) (1:4 GalA-GalA) GAUT11 (synthesizes mucilage HG)	Sterling et al (2006) Voiniciuc et al (2018)

Rhamnogalacturonan 1	P	α -D-galacturonic acid α-L-arabinan f β-D-galactose α-rhamnose	1:4 (GalA-Rha) 1:2 (Rha-GalA)	Common constituent of seed mucilage Second most abundant structural component of pectins	RRT1-4 (RHAMNOGALACTURONAN RHAMNOSYLTRANSFERASE) (GTF106) synthesize the GalA-Rha repeats MUCI70 (arabinan side chain production?) GAUT11 (HG primer required for RG1 synthesis?) RG-GalT (1:4 Gal-Rha)	Takenaka et al (2018) Voiniciuc et al (2018) Wachananawat et al (2020) Matsumoto et al (2019) Gutterman & Shemtov (1996)
Galactan	P: RG-1	β-D-galactose	1:4 Gal-Gal	Binds cellulose during cell wall assembly	GALS1 (GALACTAN SYNTHASE) (GTF92)**	Liwanag et al (2012) Zykwinska et al (2005)

Arabinan (‘type 1’)	P: RG-1	α-L-arabinan f	1:3, 1:5	Stomatal opening Binds cellulose during cell wall assembly	ARAD1/ARAD2 (ARABINAN DEFICIENT) (GTF47)	Zykwinska et al (2005)
Arabinogalactan (type 1)	P: RG-1	α-L-arabinan f β-D-galactose p	1:4 (main galactan) 1:3 (Gal-Ara) 1:5 (Gal-Ara)			Hinz et al (2005)
Rhamnogalacturonan 2 – chain A	P: RG-2	α -D-galacturonic acid β-D- galacturonic acid α-D-xylose α-D-methylxylose α-L-aceric acid f β-D-apiosef α-L-fucose p α -L-galactose p β-L-rhamnose p β-D-glucuronic acid p	1:4 (GalA-GalA) 1:2 (Gal-GlcA) 1:2 (GalA-Rha) 1:3 (GalA-Rha) 1:4 (GlcA-Fuc) 1:3 (Rha-Api) 1:2 (Api-GalA) 1:3 (MeXyl-Fuc)	Cell wall extension Borate cis-diol ester bond formation	RGXT 1:4 (RHAMNOGALACTURONAN II XYLOSYLTRANSFERASE) (GTF77) (1:3 Xyl-Fuc) (chain A) Cdi (adds galactose to chain A)*	Egelund et al (2006; 2008) O’Neill et al (2001) Peng et al (2021) Rodriguez-Carvajal et al (2003)

Rhamnogalacturonan 2 – chain B	P: RG-2	β-D-apiose α-L-rhamnose β-L-rhamnose 2-O-methyl-α-L-fucose α-L-arabinosef β-D-galactose α-L-aceric acid	1:2 (Ara-Rha) 1:2 (Rha-Ara) 1:4 (Ara-Gal) 1:2 (MeFuc-Gal) 1:2 (Gal-AceA) 1:3 (AceA-Rha) 1:3 (Rha-Api) 1:2 (Api-GalA)			Rodriguez-Carvajal et al (2003)
Rhamnogalacturonan 2 – chain C	P: RG-2	2-keto-3-deoxy-D-manno-octulosonic acid α-L-rhamnose	1:5 (Rha-Kdo) 2:3 (Kdo-GalA)		SIA1;2 (SIALYLTRANSFERASE LIKE) (GTP29) (adds Dha or Kdo) KDTA (KDO TRANSFERASE) (2:3 Kdo-GalA)	Dumont et al (2014) Séveno et al (2010) Rodriguez-Carvajal et al (2003)
Rhamnogalacturonan 2 – chain D	P: RG-2	2-keto-3-deoxy-D-lyxo-heptulosaric acid β-L-arabinose f	1:5 (Ara-Dha) 2:3 (Dha-GalA)		SIA1;2 (SIALYLTRANSFERASE LIKE) (GTF29) (adds Dha or Kdo)	Dumont et al (2014) Rodriguez-Carvajal et al (2003)

4.2 IMMUNOFLUORESCENCE ASSAYS

To verify whether Al and Si influence cell wall composition, we performed a broad immunofluorescence assay targeting components of both the pectic and the hemicellulose components of the CW. We incubated root cross-sections from Al-resistant and Al-sensitive maize lineages with rat monoclonal antibodies (MAbc) targeting arabinan, which is present in pectic and protein fractions of the CW, pectic homogalacturonan with high and low degrees of methylsterification, and xylan, which is the main component of grass hemicellulose. Results indicate that there was no visible difference in fluorescence between plants exposed to 24 or 48h of growth conditions. Therefore, all results shown here refer to the 24h experimental group.

Figure 1 shows that the two lineages exhibited different responses in arabinan content to the Al and Si treatments. None of the lineages presented detectable fluorescence in the control treatments (a, b). Only the Al-resistant lineage showed increased arabinan in the Si treatment (figure 1b), with fluorescence present mostly in the cortical region. On the other hand, a detectable response for the Al treatment was seen only in the Al-sensitive lineage (figure 1g), which had a disorganized fluorescence pattern in both the cortical and the pith regions. The Al/Si treatment in the Al-sensitive lineage presented no detectable fluorescence, as with the control (figure 1h). Interestingly, Cateto roots treated with Al/Si showed a unique fluorescence pattern in the cortical parenchyma cells (figure 1d, i), with only the proximal side (facing the pith) of the cells fluorescing.

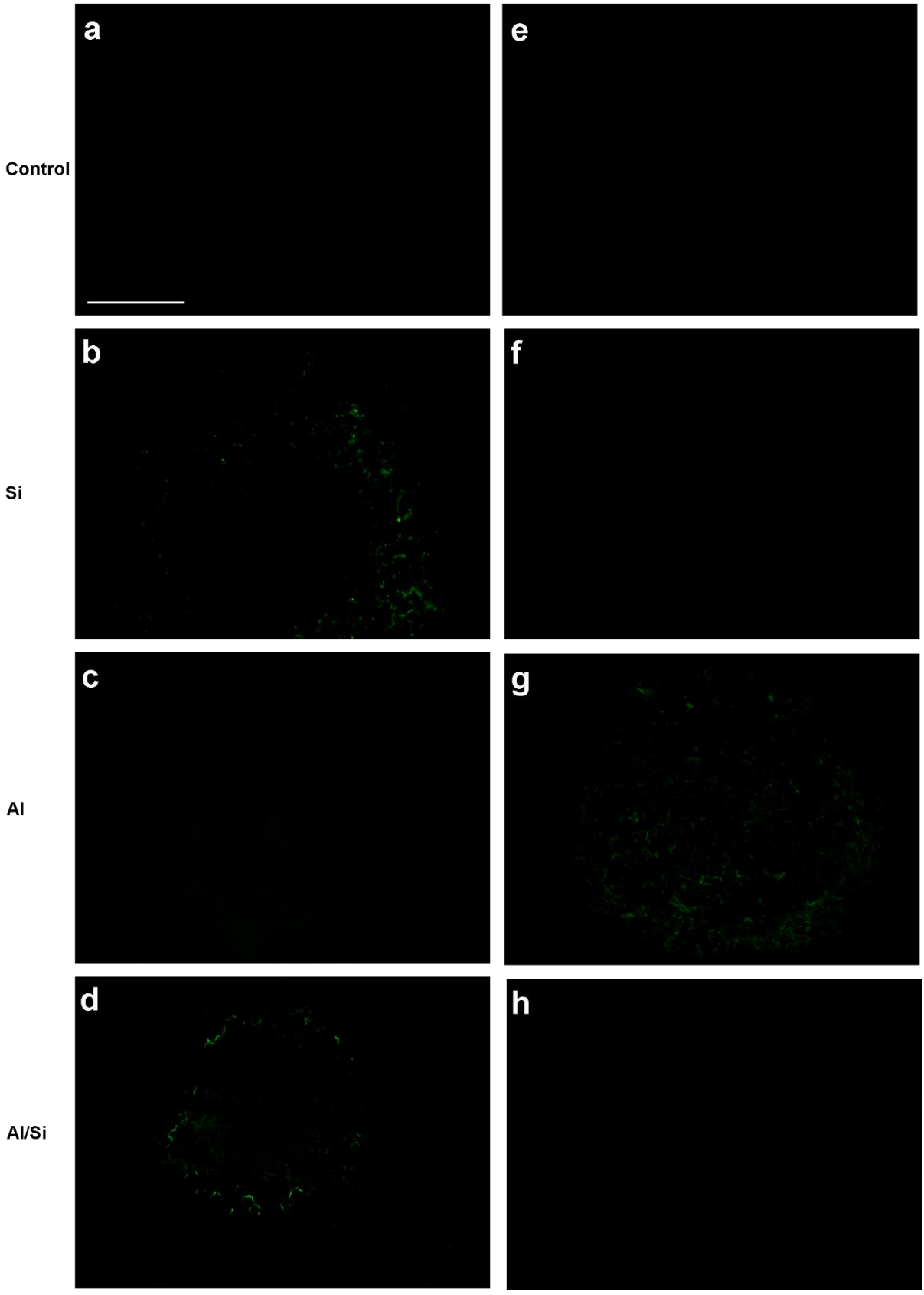
a
e
Control
b
f
Si
c
g
Al
d
h
Al/Si

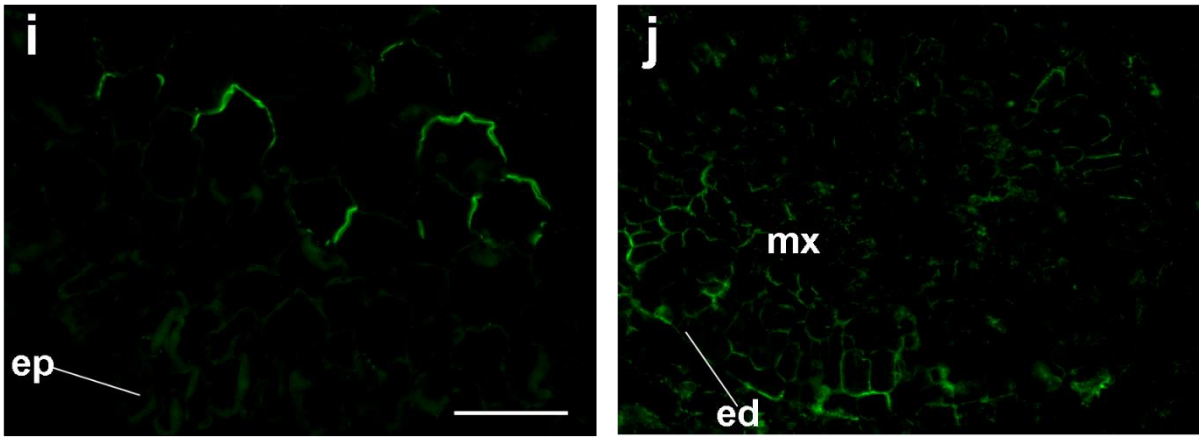

Figure 1 - immunolocalization of cell wall arabinan (LM6 epitope) in root cross sections of maize lines cateto and L53 treated with nutrient solution (a, e) and containing Si (b, f), Al (c, g), or Al and Si (d,h). (I, j) are insets of (d, g). Root sections were taken 5 – 10mm behind the apex. (a - h) scale bar: 200um. (i-j) scale bar: 100um

Detectable changes in LM10 fluorescence (xylan) occurred only in Al-treated roots of Cateto and L53 and in Al/Si-treated roots of Cateto plants. Figures 2c and i show an increase in xylan deposition restricted mostly to protoxylem cells in Al-treated Cateto roots. In contrast with the localized increase in xylan observed in Cateto roots, exhibited an increase in fluorescence in the vascular and epidermal regions (figure 2g). Al/Si treated Cateto roots showed a response similar to the Al treatment, but xylan content was also increased in the surrounding protoxylem parenchymatous tissue (figure 2d, j). There was no change in the fluorescence in pith parenchyma cells or in the surrounding metaxylem in any treatment groups. While it is difficult to locate phloem cells due to their inconspicuous shape and small size, it can be assumed that they also showed increased xylan content, assuming they are located between protoxylem cells (figure 2d, j).

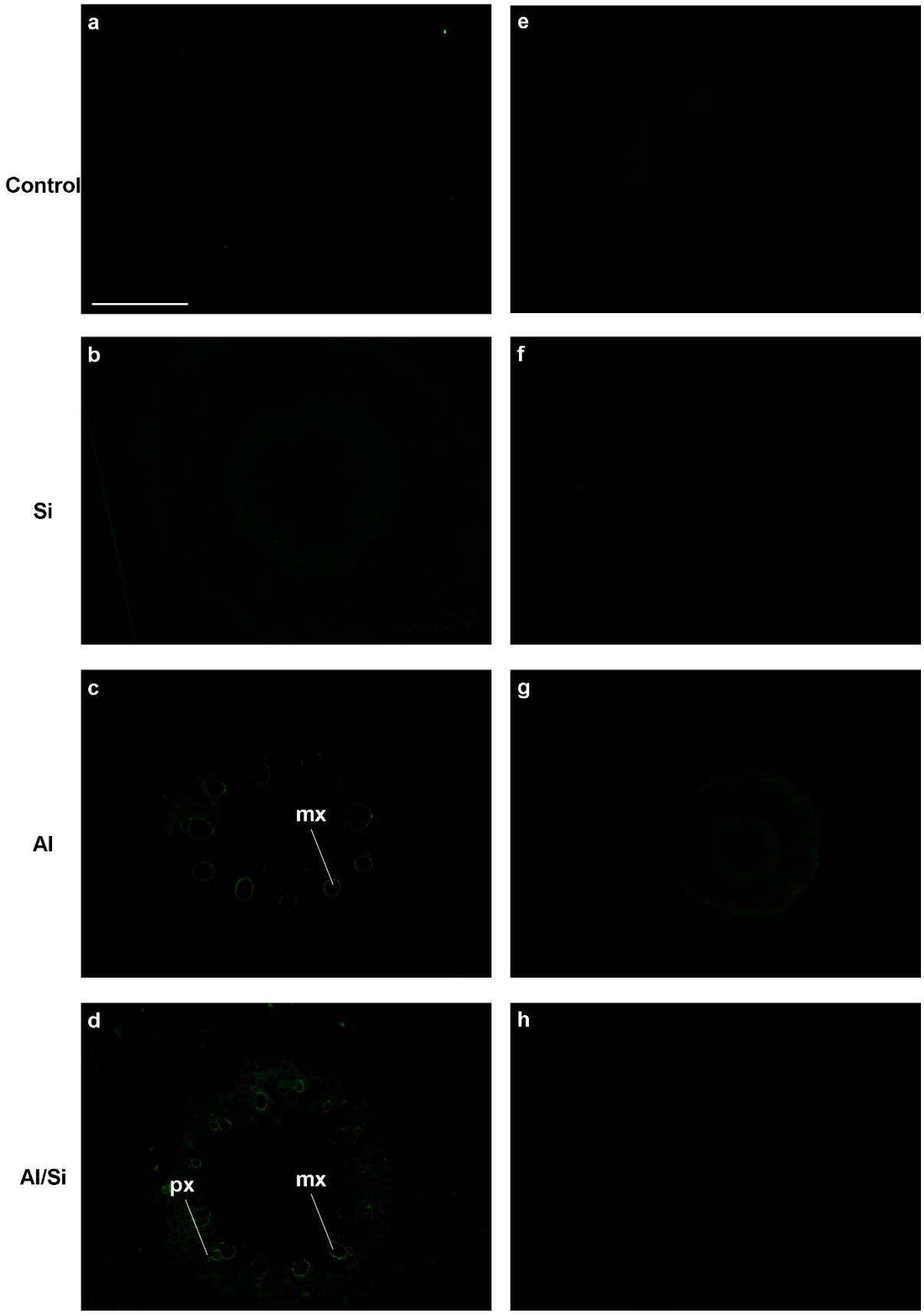
Control
Si
Al
Al/Si
a
b
c
d
e
f
g
h
mx
px
mx

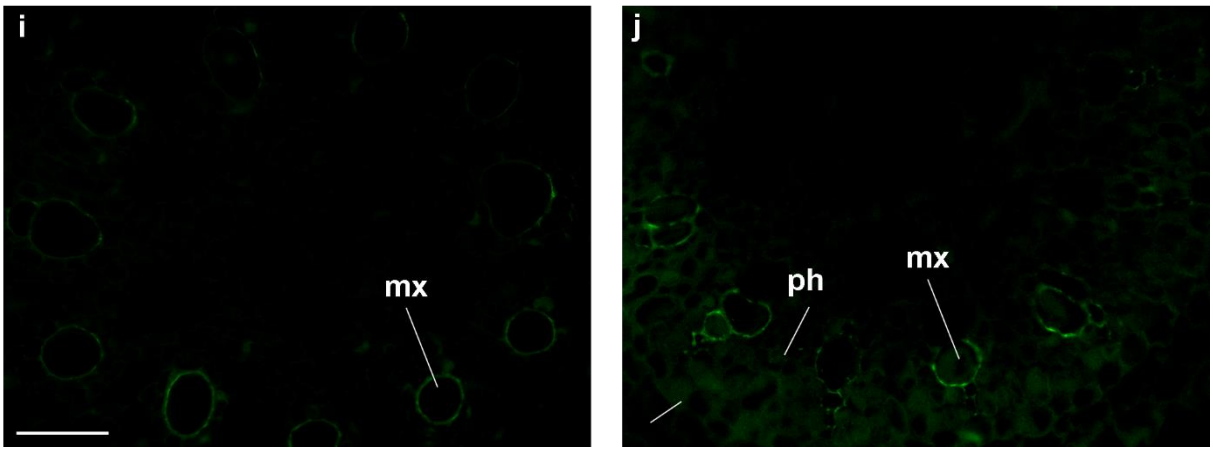

Figure 2– immunolocalization of cell wall xylan (LM10 epitope) in root cross sections of maize lines Cateto (a-d) and L53 (e-h) in control (a, e), Si (b, f), Al (c, g) and Al/Si (d, h) solutions. (i, j) are insets of (c, d). pc, pericycle; ph, phloem; px, protoxylem. (a, h) scale bar: 200um. (Insets) scale bar: 100um.

The two lineages exhibited contrasting responses in homogalacturonan methylsterification (LM19 epitope). Predictably, no roots had significant homogalacturonan content in control treatments. This is expected because monocot tissues in general have low pectin content in comparison with eudicots. Si treated roots also showed no detectable fluorescence. However, the Al-sensitive L53 lineage showed a marked increase in unsterified homogalacturonan (HG), mostly in vascular tissue (figure 3g). The Al/Si treatment also exhibited visible fluorescence, (figure 3h). Starting from the stele, different regions showed varying responses: xylem parenchyma had an increase in fluorescence, cortical tissue showed weak fluorescence in specific cells, and the epi- and hypodermal layers had higher fluorescence.

Contrastingly, an increase in highly methylsterified HG (HG-Me, LM20 epitope) was only observed in Cateto roots treated with Si or Al/Si. Si-treated roots had weak fluorescence in protoxylem cells and, less evidently, in the surrounding tissue (figure 4c). The Al/Si treatment caused an increase in fluorescence in most tissues (figure 4d). Stronger fluorescence was detected in young protoxylem than in older protoxylem cells. In addition, cells of the xylem parenchyma exhibited accumulation of HG-Me at the cellular tri-junction (figure 4j, circled areas) and also in some cells of the cortical and epidermal regions.

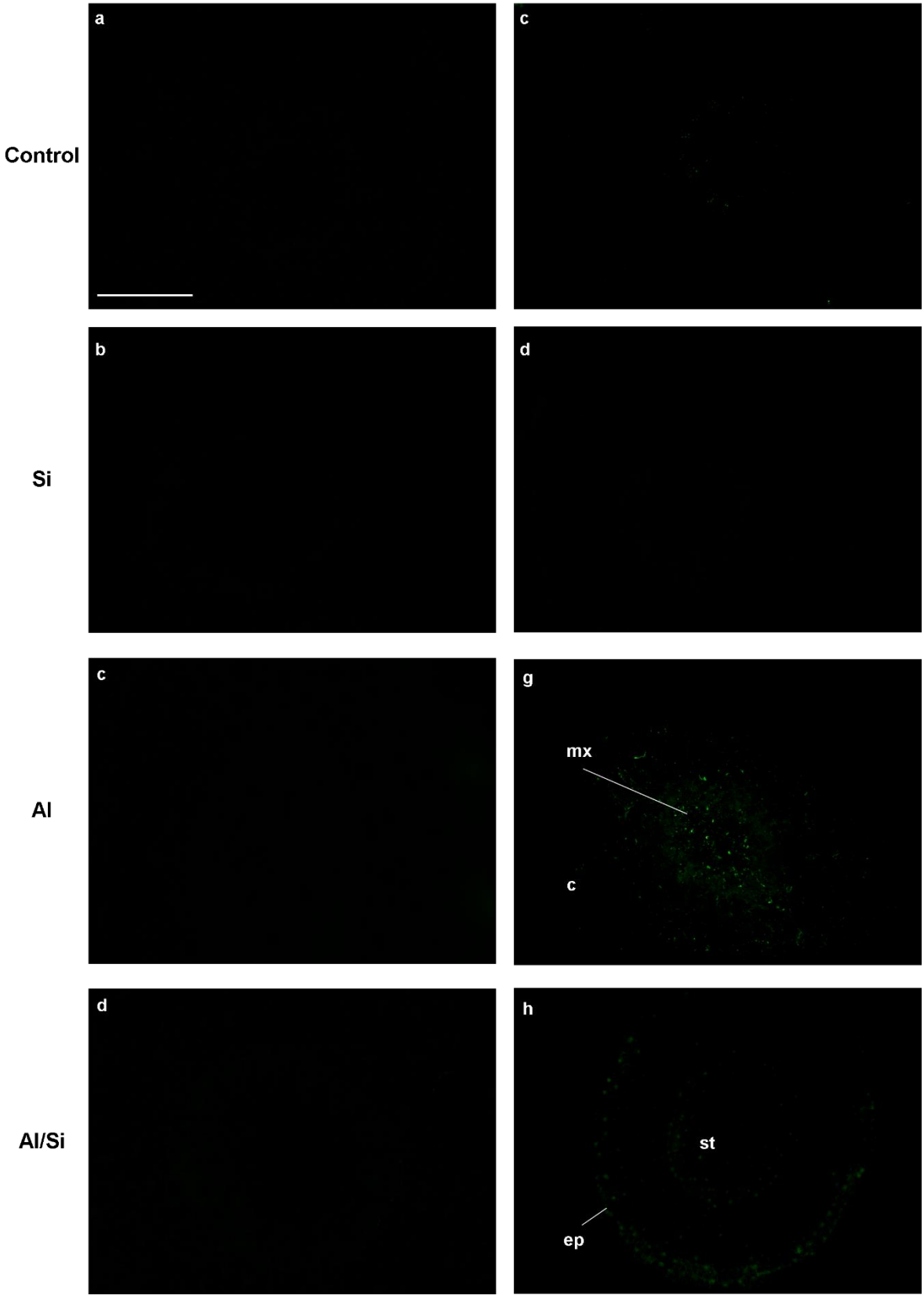

Figure 3 – immunolocalization of cell wall homogalacturonan with low methylesterification (LM19 epitope) in root cross sections of maize lines Cateto (a-d) and L53 (e-h) in control treatment (a, e), treated with Si (b, f), Al (c, g), or Al/Si (d, h). Root sections were taken 5 – 10mm behind the apex. c, cortex; ep, epidermis; mx, metaxylem; st, stele. Scale bar: 200um.

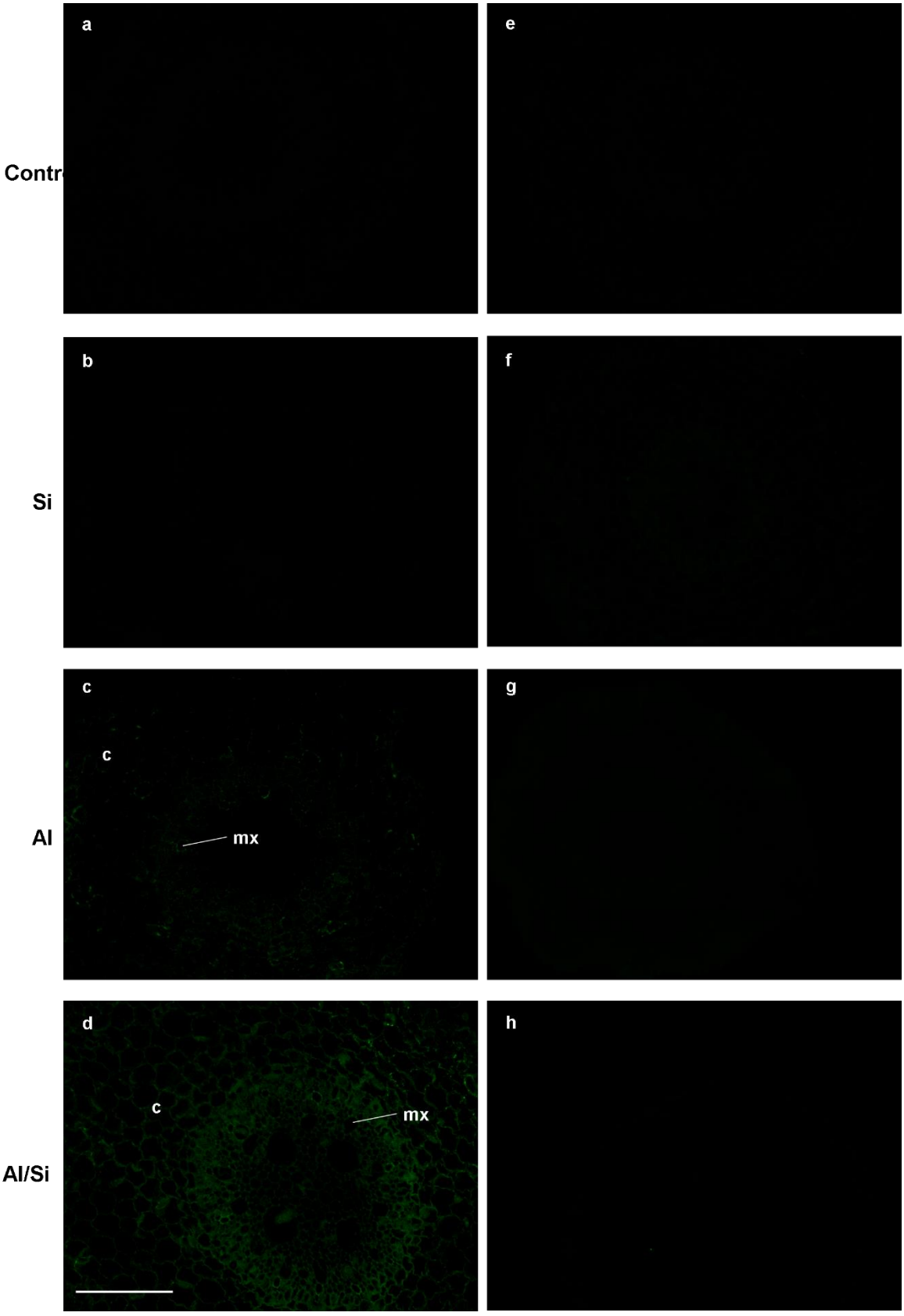
a
e
Contr
b
f
Si
c
c
mx
g
Al
d
c
mx
h
Al/Si

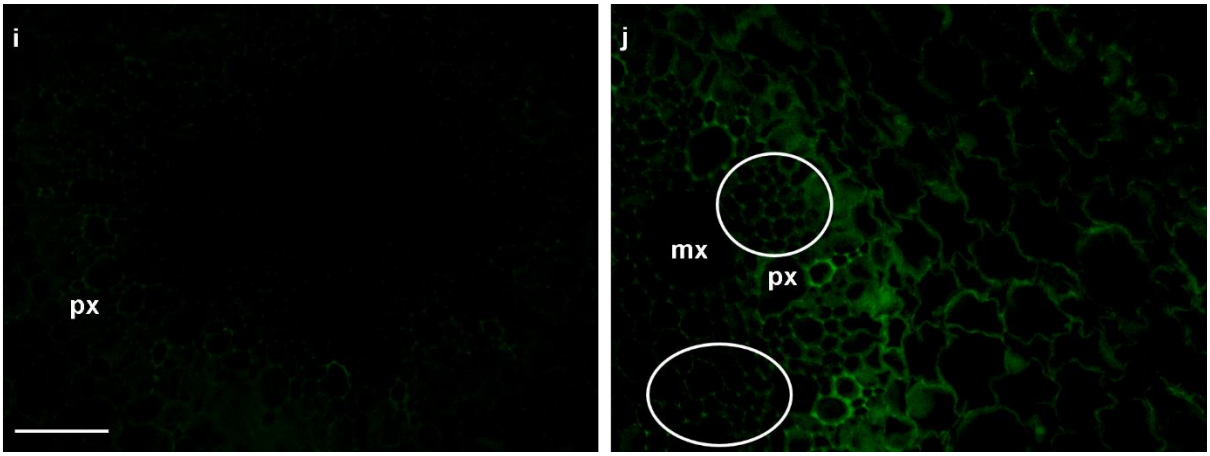

Figure 4 – immunolocalization of cell wall highly methylesterified homogalacturonan (LM20 epitope) in root cross sections of of maize lines Cateto (a-d) and L53 (e-h) in control treatment (a, e), treated with Si (b, f), Al (c, g), or Al/Si (d, h). (i, j) are insets of (c, d). Root sections were taken 5 – 10mm behind the apex. c, cortex; ep, epidermis; mx, metaxylem; st, stele. (a – h) scale bar: 200um. (Insets) scale bar: 100um.

4.3 DFT ANALYSIS

Figure 5 depicts the final optimized structure generated by the SIESTA code and visualized with Chemcraft software. The structure consists of two representative pentoses, here shown isolated from other sugars in the polymers, linked at C3 and C4 by C-O-Si bonds and Al-O bonds. In figure 6a C is represented by black atoms, H by white atoms, O by red atoms, Al by a light purple atom and Si by a beige atom. The large van der Waals radius of Al and Si (figure 6b) minimizes steric clashes between the linked pentoses. Al-O bonds are longer than Si-O bonds (figure 6c)

Simulating the interactions between Al, Si and four monomers generates a symmetrical tetramer shown in figure 6. In this scenario, Al is coordinated to four oxygen atoms, promoting the formation of a covalent bridge between the four monomers. Al is placed at the symmetrical center of the structure, and its large van der Waals radius again minimizes steric clashes between the linked monosaccharides (figure 6b). Al-O bonds are longer than Si-O bonds, therefore the structure preserves the spatial characteristics of the smaller dimer structure generated previously (figure 6c). The Al atom is slightly more negative than the Si atoms, and both are surrounded by negatively-charged O atoms.

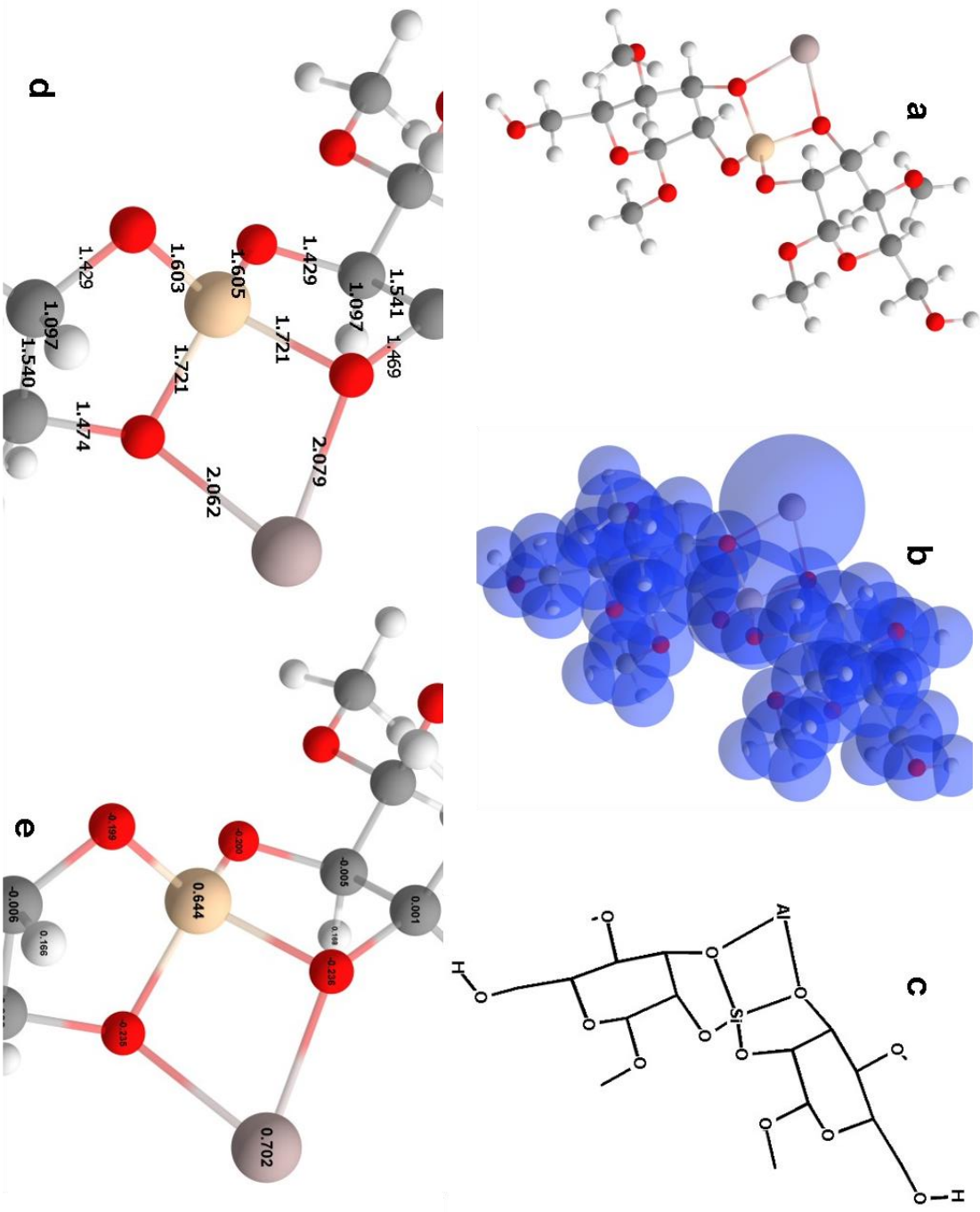

Figure 5 - proposed structure resulting from the interaction between Al, Si and two representative pentoses from two cell wall polysaccharides. Methyl ends represent sites of additional sugar linkages. (a) three-dimensional representation of the complex where carbons are black atoms, hydrogen is white, oxygen is red, aluminum is light purple and silicon is beige. (b) bond length of the interface between two monosaccharides (c) van der Waals radius of each atom. (d) two-dimensional organic notation in which hydrogen atoms are excluded to aid visualization.

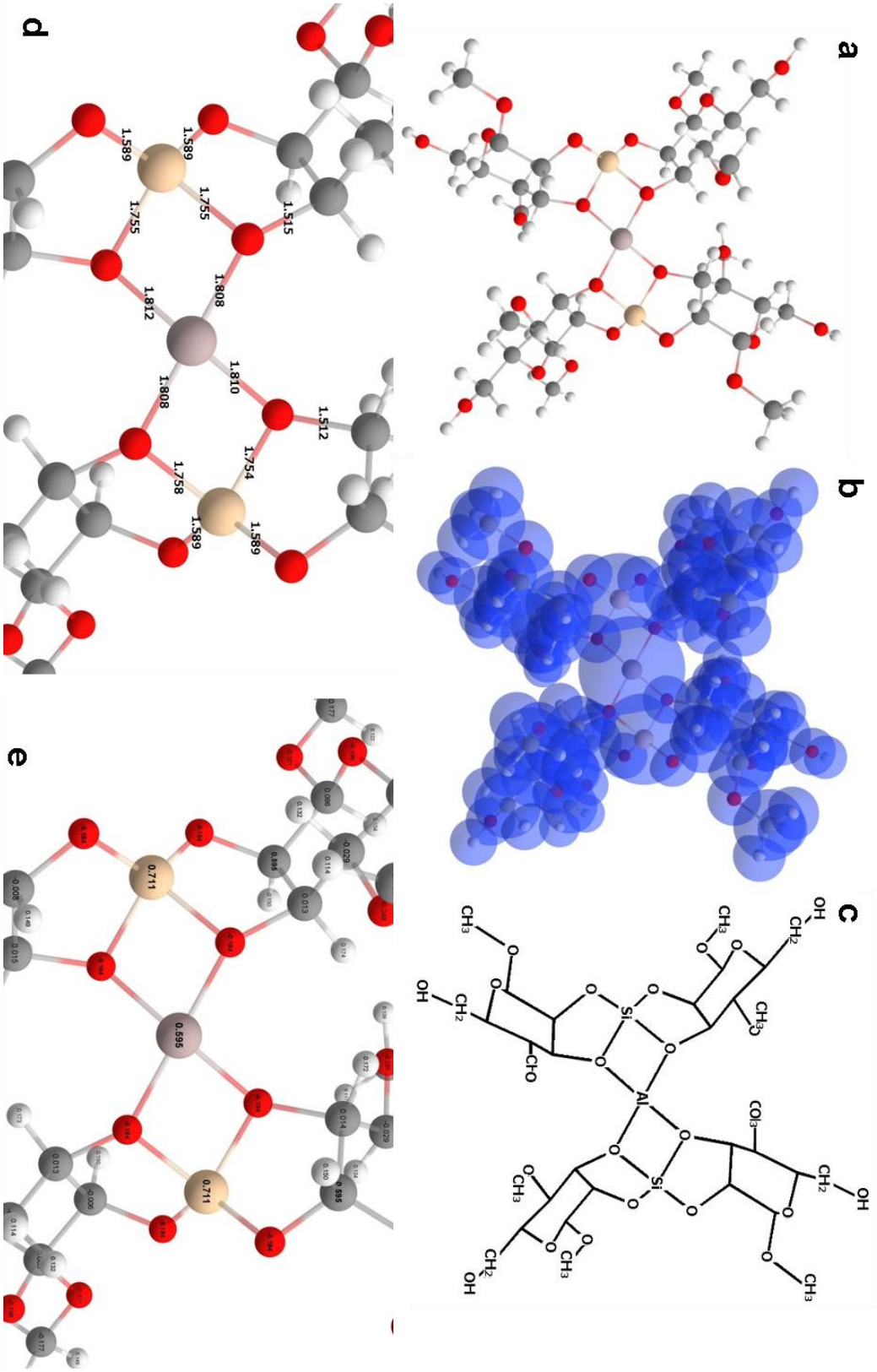

Figure 6 - proposed structure resulting from the interaction between Al, Si and four representative pentoses from four cell wall polysaccharides. (a) three-dimensional representation of the complex where carbons are black atoms, hydrogen is white, oxygen is red, aluminum is light purple and silicon is beige. (b) van der Waals radius of each atom. © bond length of the interface between the monosaccharides (d) partial charge of each atom (e) two-dimensional organic notation in which hydrogen atoms are excluded to aid visualization.

5. DISCUSSION

5.1 MOLECULAR BASIS OF CW SYNTHESIS

While great progress has been made regarding the identification of genes and proteins involved in cell wall polysaccharide synthesis, Table 2 shows there is a notable lack of information on the glycosyltransferases that synthesize pectic polymers, especially rhamnogalacturonan II, which, not coincidentally, is the most complex plant polymer identified to date. To the best of the author's knowledge, there is currently very little information on the genes and proteins involved in RGII side chain synthesis. Indeed, currently we do not know even the function of the enormous diversity of monosaccharides encountered, except for the boron diester links formed between Api residues in side-chain A. Identifying the glycosyltransferases and related proteins that synthesize these complex chains will enable further studies clarifying the function of these sugars. By using bioinformatic analysis on genes and proteins involved in RG-II synthesis, one can begin to speculate on the function of these sugars by analyzing which other genes are co-expressed and their functions.

It is estimated that over 600 proteins may be involved in CW synthesis, most of which are yet to be identified. Therefore, much more information is still needed in order to better determine the molecular basis of the CW response to Al and Si. In fact, while there is considerable interest in the physiological response of roots to Al, there are relatively few studies concerning the molecular basis of the CW response to Al, with most focusing on pectin biosynthetic genes or methylesterases and hydrolases (Schmohl et al, 2000; Yang et al, 2008; Tsutsui et al, 2012;), and not on genes involved in other CW fractions, in spite of transcriptomic analysis revealing a very significant response of general CW genes to Al (Tsutsui et al, 2012; Grisel et al, 2010). Notably, even less is known about the CW response to Si, even though its relationship with the CW has been long established, at least in grasses and some ferns (Sangster et al, 2001).

5.2 PRIMARY CW COMPONENTS RESPOND DIFFERENTIALLY TO AL AND SI IN BOTH LINEAGES

The immunofluorescence assays demonstrate that two lineages of maize, one resistant and one sensitive to Al, respond differently to Al, Si and the combined treatment of Al/Si, as summarized in Table 2. Overall, both lineages exhibited low levels of the assayed CW polysaccharides in control nutrient solutions. However, in all other treatments, each lineage responded with increases in different polysaccharides to each treatment, except for xylan, which significantly increased in both lineages in response to the Al treatment.

Arabinan changes were evident in Cateto roots treated with Si, and these changes appeared to be potentialized by the addition of Al. That is, these changes observed in Cateto roots are induced by Si and are independent of Al stress signals (figure 1b), but it appears that Al further increases arabinan content only when Si is present (figure 1d). In fact, Ruth-Maria et al (2010) showed that repressing TOR kinase, which is a major hub for controlling cell growth in response to stress signals, caused no changes in root arabinan, while modifying galactan content. It is very likely that Al represses TOR via ABA signaling (unpublished data from our lab; Fang et al, 2021). Therefore, production of arabinan appears to be independent of any Al-induced stress signals relayed by the TOR complex. In this context, our results show that there are other pathways controlling arabinan synthesis that respond to exogenous compounds, such as Si, but are unresponsive to Al stress alone. However, Si and Al may act synergistically to increase arabinan content. This implies that the interactions between Al and other elements directly affects the cell wall, further increasing the complexity of Al toxicity mechanisms in the root. In addition, the fact that arabinan content was greatly increased in Al-treated L53 roots (figure 1g) indicate that the arabinosyltransferases responsible for synthesizing pectic arabinans likely receive differential regulation between species, and even between two lineages, as shown here. So far, two proteins have been reported as arabinosyltransferases (ARABINAN DEFICIENT1/2 (Harholt et al, 2006; 2010) In response to Cd stress, two lineages of *Arabidopsis halleri* also showed contrasting activities of ARAD2 (Corso et al, 2021), further implying that arabinan synthesis does not have a conserved regulation pathway between lineages or species. This does not mean that arabinan content is irrelevant to the metal stress response in plants, since we show here that two lineages varying in Al tolerance also have different root arabinan content.

Furthermore, it is worth noting that the “half-moon” fluorescence pattern evident in figures 1d and g is similar to the expression pattern of Lsi2, which a Si efflux transporter (Ma et al, 2007). Lsi2 is expressed in the distal side of cortical cells plasma membrane in order to transport Si to the stele. If Si transporters are upregulated only when both Al and Si are present (Pontigo et al, 2017), the possibility that arabinan synthesis and Si transport share regulation pathways cannot be excluded. However, the functional relation between them, if there is any, remains unclear. Therefore, further studies evaluating gene expression of Lsi2 on these lineages are necessary to characterize its response to Al and Si.

Al and Si also appeared to have synergistic effects on xylan content of Cateto roots (figure 2c, d). However, unlike the arabinan response, Al seems to induce a primary response which is

enhanced by Si. Al greatly stimulates xylan deposition especially in protoxylem cells. Recently, a study conducted by Dong et al (2020) demonstrated the existence of a transcription factor in maize that affects protoxylem cell wall synthesis named NECROTIC UPPER TIPS 1 (NUT1). This transcription factor localizes specifically in the nucleus of nascent protoxylem cells and appears to stimulate xylan deposition. Taking this work into account, the results in figures 5a and b indicate that Al stress may upregulate NUT1, or other related transcription factors orthologs to the VND (VASCULAR RELATED NAC-DOMAIN proteins that act on xylem differentiation) subfamily to induce xylan deposition. It should be noted that there are other transcription factors directly controlling IRX glycosyltransferases, such as KNAT7 in Arabidopsis (He et al, 2018), which may be involved in stimulating xylan deposition in other regions of the stele, as observed in this work. However, NUT1 seems a likely candidate for regulating Al-induced xylan deposition in protoxylem, since it localizes specifically in these cells, and responds to other abiotic stresses. It also remains to be seen whether Si has any effect on the expression of Al-resistance genes associated with the CW.

Several studies have aimed to unravel the mechanisms and regulation of xylan synthesis and deposition in plants. These mechanisms have important applications in biotechnology as xylan is recalcitrant to fermentation and therefore is undesirable in the production of ethanol and other fermentation products. In addition, xylan deposition is part of lignification, which further increases biomass recalcitrance. Some MYB transcription factors have been implicated in the co-regulation of xylan and lignin biosynthetic genes (Yang et al, 2017; Ma & Constabel, 2019). In fact, PdMYB221 regulates the expression of most genes related to monolignol synthesis, from upstream (such as *phenylalanine ammonia lyase*) to downstream genes (such as *cinnamyl alcohol dehydrogenase*), as well as the main genes related to the xylan biosynthetic complex (Tang et al, 2015). Petersen et al (2012) is an example of an extensive research project aiming to manipulate xylan biosynthesis to improve plant biomass potential for second-generation ethanol production. The results shown here implicate that Al increases xylan content in tissues. This may impact the productivity of crops cultivated in tropical regions, since Al is present in significant amounts in *oxisols*, which is the most abundant soil family in neotropical regions. The ability to improve the productivity of tropical crops destined to fermentation may thus depend on further clarifying the relationship between Al toxicity and xylan content. In fact, reducing the content of non-fermentable polysaccharides in sugarcane is one of the objectives of a coordinated effort in Brazil led by the Bioethanol National Institute of Science and Technology (INCT Bioetanol), which aims to produce cell wall-derived ethanol.

The Al-sensitive L53 lineage showed a significant increase in unmethylsterified HG. In general, unmethylsterified HG is seen as an undesirable trait for Al-tolerance, since the exposed carboxyl groups, which are ionized at cellular pHs, may adsorb positively-charged Al^{3+} and therefore contribute to an increase in overall Al concentration in the roots (Yang et al, 2008). In addition, figure 3g shows disorganization of cell shape and HG deposition in the stele of Al-treated roots, which may be a symptom of increased Al toxicity. Interestingly, treatment with Al/Si further increased fluorescence, which can be detected even in the outer/epidermal layers of the root (figure 3h). This is possibly not a well-adapted response to Al stress because an increase in unmethylsterified HG at the epidermis could facilitate Al uptake by the roots. Most characterized or putative transporters that mediate Al uptake by the roots are members of the Nodulin 26-like Intrinsic Protein family and the aquaporin (AQP) subfamily (Wang et al, 2017; Xia et al, 2010; Negishi et al, 2012; Negishi et al, 2013). Aquaporins (and NIPs in general) are passive transporters (Pomerrenig et al, 2015), therefore an increase in root negative charges directly facilitates the flow of Al cations into the cells.

Highly methylsterified pectins accumulate at the "tri-junctions" between vascular cells of Cateto roots treated with Al and Al/Si (figure 4c, d). This is unusual because these corners have a role in promoting cell adhesion, and many studies have shown that to fulfill such role they contain greater levels of low or unmethylsterified HG (Parker et al., 2001; McCartney and Knox, 2002; Guillemin et al., 2005) in order to promote calcium crosslinking between polysaccharides. Al has been shown to disrupt and substitute such calcium bridges, further stiffening the wall and preventing elongation (Ma et al, 2004) One study involving pea root nodules, which are sensitive to Al, showed that low methylsterified pectin levels increased at the "tri-junctions"during Al exposure (Sujkowska-Rybkowska & Borucki, 2015). The results shown in figure 5 support the traditional view that Al-tolerant lineages have higher levels of HG-Me, but also show the unusual accumulation of these polymers in cell corners, which may further prevent stiffening of the wall and also alter mechanical properties of the tissue as a whole, considering the role of these junctions in promoting tissue cohesion and cell-to-cell adhesion (Daher & Braybook 2015).

Taken together, the results in figures 1, 3 and 4 point to an important role of Si in mediating or enhancing the stress response to Al in Cateto roots. Fluorescence levels in root arabinan, xylan and HG-Me was higher when both elements were present in the nutrient solution, when compared to roots treated only with Al or Si.

Lignin deposition has also been associated with Al toxicity in roots (Sasaki & Matsumoto,

1996). Since lignin is only deposited after cell growth and elongation have ceased, Al-treated roots show increased lignin content and, therefore, inhibition of elongation. Studying alfafa cell walls, Wi et al (2005) demonstrated that lignin and pectin co-localize to the middle lamella in alfafa, especially in cell corners, which are generally seen as the start sites of monolignol polymerization. Furthermore, in vitro experiments conducted by Lairez et al (2005) show that coniferyl alcohol, which forms the guaiacyl units of lignin, polymerizes and aggregates with pectin. The accumulation of pectin in cell corners in Al+Si treated (fig. 4j) shown here would, therefore, favor lignin deposition. This is inconsistent with the Al-tolerant characteristics of the Cateto lineage and with the beneficial aspects of Si uptake. One possible explanation is that, since Cateto roots accumulate only HG-Me, lignin interactions would not be favored due to the unavailability of polar carboxyl groups capable of interacting with hydroxyl ends of monolignol units. Supporting this hypothesis, some studies (Carpin et al, 2001; Dunand et al, 2002) showed that peroxidases, which are, along with laccases, responsible for the polymerization of lignin, may need to be anchored to calcium cross-linked, that is, unsterified HG to catalyze their reactions. However, it remains to be seen what is the relationship between specific pectic polysaccharides, such as HG and HG-Me, and lignins.

5.3 DFT SIMULATED STRUCTURES SHOW THE FORMATION OF STABLE COMPLEXES BETWEEN POLYSACCHARIDES, AL AND SI

The immunofluorescence results show that Si and Al, when applied together, magnify the CW changes exhibited when either are present alone. These data imply that both elements together promote structural changes in the cell wall, possibly by promoting the formation of stable complexes between CW sugars. To confirm this hypothesis, we used Density Functional Theory, an analytical method based on quantum physics, to simulate the interactions between Si, Al and representative pentoses from the CW. In the first scenario, we simulated the interactions between the elements and two pentoses, each from a separate polysaccharide. A dimer-like structure was generated, with Si bonded by organosilicon linkages at C3 and C4 which unite the sugar monomers (figure 5), leaving C1 and C5 free to establish glycosidic bonds with other sugars. Here, Al attacks the negatively-charged oxygen atoms bonded to Si and establishes additional Al-O bonds. As shown in figure 5d, the presence of Al introduces a ‘kink’ in the structure, which would likely result in a spiral-like shape in a longer molecule of this type. Therefore, the Si/Al/sugar structure would have a very different spatial organization compared to a hemicellulosic polymer, which are usually linear due to their beta 1,4 glycosyidic

bonds. Given the positive charge of the Al atom when bound to this structure (figure 5e), we decided to investigate the possibility of additional sugars being linked to the Al atom via electronegative oxygen atoms. This is shown in figure 6, which shows the interactions between Al/Si and four monomers from four polysaccharides from the CW. In this case, a large, symmetrical tetramer-like structure was generated, in which Al is at the center, connecting the four monomers. The bonds between Al and O are, at over 2A in length, quite long, enabling the four bulky sugar moieties to exist further apart from each other, minimizing steric clashes and increasing stability. Overall, given its symmetric features and extensive bonding between the sugar portions provided by the Si/Al portion, this complex, if confirmed in planta, would significantly stabilize the CW, promoting the formation of stronger, covalent-like bonds in addition to the weaker hydrogen bonds and van der Waals interactions which usually link and stabilize adjacent polysaccharides. This would have major implications for the CW. First, the formation of the complex would signify that, in the presence of Si, Al can bind to the CW, at the same time preventing its diffusion to the symplast and increasing CW stability. In this sense, Si and Al, when present at the same time in plant tissues, are more beneficial to the plant than when each is applied separately. Thus, the synergistic effects shown in the immunofluorescence assays would be explained by the physical interactions between Si and Al in the CW. The plant may synthesize more CW polysaccharides in order to (1) immobilize Al in the apoplast and (2) increase CW stability and interactions between adjacent polymers. Therefore, these results challenge the traditional view of Al as a solely toxic element, since we show here possibly beneficial effects of Al when present with Si in the cell wall. However, it is important to note that these in silico simulations must be confirmed through, at least, in vitro studies. Currently, available techniques, such as Atomic Force Microscopy (AFM), Nuclear Magnetic Resonance (NMR) and Mass Spectrometry (MS) do not allow for detailed evaluations of the spatial organization and interactions of polymers in the cell wall, therefore in silico experiments provide valuable data regarding chemical interactions in this environment. In addition, it would be interesting to investigate the consequences of the formation of this complex for the process of cell expansion and CW elongation.

8. CONCLUSIONS

The results shown in this work indicate that Al and Si have visible and remarkable effects on the composition of the cell wall of maize roots. Immunofluorescence assays demonstrate that the exposure to Al or Si alone, or both, produce distinct effects each on cell wall composition. Al-resistant Cateto roots exhibited a distinct response from Al-sensitive L53 roots. In general,

treatment with Al and Si significantly increased deposition of arabinan, xylan and HG-Me in the Al-resistant lineage. Each of these polymers was deposited in a unique pattern, contrasting with the Al-sensitive response, which exhibited disorganized deposition of arabinan and low methylesterified HG. However, it is not possible with these results to link polysaccharide deposition with increased or decreased resistance to Al. Molecular and genetic studies are needed to clearly demonstrate the importance of each polymer investigated here for Al resistance or tolerance. In addition, results indicate that Al and Si may act synergystically on the cell wall, given the stronger fluorescence levels reported on treatments with Al and Si. This hypothesis is supported by DFT analysis results, which produced a stable and symmetric complex between Al, Si and hemicelluloses which may help stabilize the cell wall under stress conditions.

These results indicate that there are still many unknown aspects regarding the physiological importance of Al and Si. Given their abundance and co-occurrence in soils, it is likely that there may be shared or interdependent molecular pathways controlling the plant response to these elements. Elucidating the complex effects of these elements in plants is a necessary step in improving agriculture worldwide, but especially in developing countries situated in the tropics.

Table 3 - summary of observed changes in fluorescence in LM6, LM10, LM19 and LM20 Mabcs (targeting arabinan, xylan, unsterified and high methylsterified homogalacturonan, respectively) of *Zea mays* cvs. Cateto and L53.

Lineage/treatment	Cateto	L53
Control	-	-
Si 24h	LM6, LM20	-
Si 48h	LM6, LM20	-
Al 24h	LM10	LM6, LM10, LM19
Al 48h	LM10	LM6, LM10, LM19
Al/Si 24h	LM6, LM10, LM20	LM19
Al/Si 48h	LM6, LM10, LM20	LM19

REFERENCES

ABEDIN, Mohammed Joinal; FELDMANN, Jorg; MEHARG, Andy A. Uptake kinetics of arsenic species in rice plants. **Plant physiology**, v. 128, n. 3, p. 1120-1128, 2002.

ALBERSHEIM, Peter et al. **Plant cell walls**. Nova York: Garland Science, 2011.

ARENHART, Rafael Augusto et al. Involvement of ASR genes in aluminium tolerance mechanisms in rice. **Plant, Cell & Environment**, v. 36, n. 1, p. 52-67, 2013.

ARROYO-SERRALTA, Gabriela A. et al. Exposure to toxic concentrations of aluminum activates a MAPK-like protein in cell suspension cultures of Coffea arabica. **Plant Physiology and Biochemistry**, v. 43, n. 1, p. 27-35, 2005.

ATMODJO, Melani A. et al. Galacturonosyltransferase (GAUT) 1 and GAUT7 are the core of a plant cell wall pectin biosynthetic homogalacturonan: galacturonosyltransferase complex. **Proceedings of the National Academy of Sciences**, v. 108, n. 50, p. 20225-20230, 2011.

BALDO, Brian A.; TOVEY, Euan R.; FORD, Stephen A. Comparison of different blocking agents and nitrocellulose in the solid phase detection of proteins by labelled antisera and protein A. **Journal of biochemical and biophysical methods**, v. 12, n. 5-6, p. 271-279, 1986.

BARCELO, Juan; POSCHENRIEDER, Charlotte. Fast root growth responses, root exudates, and internal detoxification as clues to the mechanisms of aluminium toxicity and resistance: a review. **Environmental and Experimental Botany**, v. 48, n. 1, p. 75-92, 2002.

BARRETO, Rafael Ferreira et al. Silicon alleviates ammonium toxicity in cauliflower and in broccoli. **Scientia Horticulturae**, v. 225, p. 743-750, 2017.

BHOOMIKA, Kumari; PYNGROPE, Samantha; DUBEY, R. S. Differential responses of antioxidant enzymes to aluminum toxicity in two rice (Oryza sativa L.) lineages with marked presence and elevated activity of Fe SOD and enhanced activities of Mn SOD and catalase in aluminum tolerant lineage. **Plant growth regulation**, v. 71, n. 3, p. 235-252, 2013.

BRADY, N. C. WEIL, R. R. Elementos da natureza e propriedades dos solos. 3 ed. Porto Alegre: Bookman, 2013. 686p.

BURTON, Rachel A. et al. Cellulose synthase-like CslF genes mediate the synthesis of cell wall (1, 3; 1, 4)-ß-D-glucans. **Science**, v. 311, n. 5769, p. 1940-1942, 2006.

CAFFALL, Kerry Hosmer. Expression and characterization of galacturonosyltransferase-6 (GAUT6) of the galacturonosyltranserferase-1 (GAUT1)-related gene family of Arabidopsis thaliana. 2008. Tese de Doutorado. University of Georgia.

CARPIN, Sabine et al. Identification of a Ca2+-pectate binding site on an apoplastic peroxidase. **The Plant Cell**, v. 13, n. 3, p. 511-520, 2001.

CHEN, Daoqian et al. Silicon-moderated K-deficiency-induced leaf chlorosis by decreasing putrescine accumulation in sorghum. **Annals of Botany**, v. 118, n. 2, p. 305-315, 2016.

COOKE, Julia; LEISHMAN, Michelle R. Consistent alleviation of abiotic stress with silicon addition: a meta-analysis. **Functional Ecology**, v. 30, n. 8, p. 1340-1357, 2016.

CORSO, Massimiliano et al. Adaptation of Arabidopsis halleri to extreme metal pollution through limited metal accumulation involves changes in cell wall composition and metal homeostasis. **New Phytologist**, v. 230, n. 2, p. 669-682, 2021.

DAHER, Firas Bou; BRAYBROOK, Siobhan A. How to let go: pectin and plant cell adhesion. **Frontiers in plant science**, v. 6, p. 523, 2015.

DELHAIZE, Emmanuel et al. Engineering high-level aluminum tolerance in barley with the ALMT1 gene. **Proceedings of the National Academy of Sciences**, v. 101, n. 42, p. 15249-15254, 2004.

DESHMUKH, Rupesh; BÉLANGER, Richard R. Molecular evolution of aquaporins and silicon influx in plants. **Functional Ecology**, v. 30, n. 8, p. 1277-1285, 2016.

DOEBLEY, John. The genetics of maize evolution. **Annu. Rev. Genet.**, v. 38, p. 37-59, 2004.

DONG, Zhaobin et al. Necrotic upper tips1 mimics heat and drought stress and encodes a protoxylem-specific transcription factor in maize. **Proceedings of the National Academy of Sciences**, v. 117, n. 34, p. 20908-20919, 2020.

DUNAND, Christophe et al. Identification and characterisation of Ca2+-pectate binding peroxidases inArabidopsis thaliana. **Journal of Plant Physiology**, v. 159, n. 11, p. 1165-1171, 2002.

EPSTEIN, E. (1990) in McGraw-Hill Yearbook of Science and Technology (McGraw-Hill, New York), pp. 315- 316.

EPSTEIN, Emanuel. The anomaly of silicon in plant biology. **Proceedings of the National Academy of Sciences**, v. 91, n. 1, p. 11-17, 1994.

ESTEBAN, Raquel et al. Mechanisms of ammonium toxicity and the quest for tolerance. **Plant Science**, v. 248, p. 92-101, 2016.

FANG, Qiu et al. Degradation of STOP1 mediated by the F-box proteins RAH1 and RAE1 balances aluminum resistance and plant growth in Arabidopsis thaliana. **The Plant Journal**, v. 106, n. 2, p. 493-506, 2021.

FREW, Adam et al. Silicon reduces herbivore performance via different mechanisms, depending on host–plant species. **Austral Ecology**, v. 44, n. 6, p. 1092-1097, 2019.

GILLE, Sascha et al. Deep sequencing of voodoo lily (Amorphophallus konjac): an approach to identify relevant genes involved in the synthesis of the hemicellulose glucomannan. **Planta**, v. 234, n. 3, p. 515-526, 2011.

GREGER, Maria; LANDBERG, Tommy; VACULÍK, Marek. Silicon influences soil availability and accumulation of mineral nutrients in various plant species. **Plants**, v. 7, n. 2, p. 41, 2018.

GOUBET, Florence et al. Cell wall glucomannan in Arabidopsis is synthesised by CSLA glycosyltransferases, and influences the progression of embryogenesis. **The Plant Journal**, v. 60, n. 3, p. 527-538, 2009.

GUILLEMIN, Florence et al. Distribution of pectic epitopes in cell walls of the sugar beet root. **Planta**, v. 222, n. 2, p. 355-371, 2005.

HARHOLT, Jesper et al. ARAD2 is a putative arabinan arabinosyltransferase and is involved in complex formation with ARAD1. In: **XIIth Cell Wall Meeting**. 2010.

HARTLEY, Susan E.; DEGABRIEL, Jane L. The ecology of herbivore-induced silicon defences in grasses. **Functional Ecology**, v. 30, n. 8, p. 1311-1322, 2016.
HE, Jun-Bo et al. KNAT7 positively regulates xylan biosynthesis by directly activating IRX9 expression in Arabidopsis. **Journal of integrative plant biology**, v. 60, n. 6, p. 514-528, 2018.

HINZ, Sandra WA et al. Type I arabinogalactan contains β-D-Galp-(1→ 3)-β-D-Galp structural elements. **Carbohydrate research**, v. 340, n. 13, p. 2135-2143, 2005.

HÖFTE, Herman; PEAUCELLE, Alexis; BRAYBROOK, Siobhan. Cell wall mechanics and growth control in plants: the role of pectins revisited. **Frontiers in plant science**, v. 3, p. 121, 2012.

HUANG, Chao-Feng et al. A tonoplast-localized half-size ABC transporter is required for internal detoxification of aluminum in rice. **The Plant Journal**, v. 69, n. 5, p. 857-867, 2012.

HUANG, Wenjing et al. Reactive oxygen species burst induced by aluminum stress triggers mitochondria-dependent programmed cell death in peanut root tip cells. **Plant Physiology and Biochemistry**, v. 82, p. 76-84, 2014.

IUCHI, Satoshi et al. Zinc finger protein STOP1 is critical for proton tolerance in Arabidopsis and coregulates a key gene in aluminum tolerance. **Proceedings of the National Academy of Sciences**, v. 104, n. 23, p. 9900-9905, 2007.

JASKOWIAK, Joanna et al. Aluminum alters the histology and pectin cell wall composition of barley roots. **International journal of molecular sciences**, v. 20, n. 12, p. 3039, 2019.

JONES, Louise; SEYMOUR, Graham B.; KNOX, J. Paul. Localization of pectic galactan in tomato cell walls using a monoclonal antibody specific to (1 [->] 4)-[beta]-D-galactan. **Plant physiology**, v. 113, n. 4, p. 1405-1412, 1997.

JONES, David L.; KOCHIAN, Leon V. Aluminum inhibition of the inositol 1, 4, 5-trisphosphate signal transduction pathway in wheat roots: a role in aluminum toxicity?. **The Plant Cell**, v. 7, n. 11, p. 1913-1922, 1995.

KEEGSTRA, Kenneth; WALTON, Jonathan. β-Glucans--brewer's bane, dietician's delight. **Science**, v. 311, n. 5769, p. 1872-1873, 2006.

KOSTIC, Ljiljana et al. Silicon increases phosphorus (P) uptake by wheat under low P acid soil conditions. **Plant and Soil**, v. 419, n. 1, p. 447-455, 2017.

LAIREZ, D. et al. Aggregation during coniferyl alcohol polymerization in pectin solution: a biomimetic approach of the first steps of lignification. Biomacromolecules, v. 6, n. 2, p. 763-774, 2005.

LEIBER, Ruth-Maria et al. The TOR pathway modulates the structure of cell walls in Arabidopsis. **The Plant Cell**, v. 22, n. 6, p. 1898-1908, 2010.

LI, Ge Zi et al. Transcription factor WRKY 22 promotes aluminum tolerance via activation of Os FRDL 4 expression and enhancement of citrate secretion in rice (Oryza sativa). **New Phytologist**, v. 219, n. 1, p. 149-162, 2018.

LIANG, Yongchao et al. Exogenous silicon (Si) increases antioxidant enzyme activity and reduces lipid peroxidation in roots of salt-stressed barley (Hordeum vulgareL.). **Journal of plant physiology**, v. 160, n. 10, p. 1157-1164, 2003.

LIANG, Yongchao et al. Effect of exogenous silicon (Si) on H+-ATPase activity, phospholipids and fluidity of plasma membrane in leaves of salt-stressed barley (Hordeum vulgare L.). **Environmental and Experimental Botany**, v. 57, n. 3, p. 212-219, 2006.

LI-FENG A, G. A. O.; SHUANG-XI B, XIONG; WEI, L. O. N. G. Density functional theory investigation of acyclovir [J]. **Chemical Engineer**, v. 7, 2013.

LIN, Yibin et al. Deficiency in silicon transporter Lsi1 compromises inducibility of anti-herbivore defense in rice plants. **Frontiers in plant science**, v. 10, p. 652, 2019.

LOMBARD, Vincent et al. The carbohydrate-active enzymes database (CAZy) in 2013. **Nucleic acids research**, v. 42, n. D1, p. D490-D495, 2014.

MAGALHAES, Jurandir V. et al. A gene in the multidrug and toxic compound extrusion (MATE) family confers aluminum tolerance in sorghum. **Nature genetics**, v. 39, n. 9, p. 1156-1161, 2007.

MA, Dawei; CONSTABEL, C. Peter. MYB repressors as regulators of phenylpropanoid metabolism in plants. **Trends in plant science**, v. 24, n. 3, p. 275-289, 2019.
MA, Jian Feng et al. Molecular mapping of a gene responsible for Al-activated secretion of citrate in barley. **Journal of Experimental Botany**, v. 55, n. 401, p. 1335-1341, 2004.

MA, Jian Feng et al. An efflux transporter of silicon in rice. **Nature**, v. 448, n. 7150, p. 209-212, 2007.

MA, Jian Feng et al. Transporters of arsenite in rice and their role in arsenic accumulation in rice grain. **Proceedings of the National Academy of Sciences**, v. 105, n. 29, p. 9931-9935, 2008.

MA, Jian Feng; YAMAJI, Naoki. A cooperative system of silicon transport in plants. **Trends in Plant Science**, v. 20, n. 7, p. 435-442, 2015.

MABAGALA, F. S. et al. Effect of silicon on crop yield, and nitrogen use efficiency applied under straw return treatments. **Applied Ecology And Environmental Research**, v. 18, n. 4, p. 5577-5590, 2020.

MARTENS, Eric C. et al. Recognition and degradation of plant cell wall polysaccharides by two human gut symbionts. **PLoS biology**, v. 9, n. 12, p. e1001221, 2011.

MARON, Lyza G. et al. Two functionally distinct members of the MATE (multi-drug and toxic compound extrusion) family of transporters potentially underlie two major aluminum tolerance QTLs in maize. **The Plant Journal**, v. 61, n. 5, p. 728-740, 2010.

MCCARTNEY, Lesley; KNOX, J. Paul. Regulation of pectic polysaccharide domains in relation to cell development and cell properties in the pea testa. **Journal of experimental botany**, v. 53, n. 369, p. 707-713, 2002.

MCCARTNEY, Lesley; MARCUS, Susan E.; KNOX, J. Paul. Monoclonal antibodies to plant cell wall xylans and arabinoxylans. **Journal of Histochemistry & Cytochemistry**, v. 53, n. 4, p. 543-546, 2005.

MEHARG, Andrew A.; RAHMAN, Md Mazibur. Arsenic contamination of Bangladesh paddy field soils: implications for rice contribution to arsenic consumption. **Environmental science & technology**, v. 37, n. 2, p. 229-234, 2003.

MIYASAKA, Susan C. et al. Mechanism of aluminum tolerance in snapbeans: root exudation of citric acid. **Plant physiology**, v. 96, n. 3, p. 737-743, 1991.

MOUSTACAS, Anne-Marie et al. Pectin methylesterase, metal ions and plant cell-wall extension. The role of metal ions in plant cell-wall extension. **Biochemical journal**, v. 279, n. 2, p. 351-354, 1991.

MUNNÉ-BOSCH, S.; JUBANY-MARÍ, T.; ALEGRE, L. Drought-induced senescence is characterized by a loss of antioxidant defences in chloroplasts. **Plant, Cell & Environment**, v. 24, n. 12, p. 1319-1327, 2001.

NEGISHI, Takashi et al. Tonoplast-and plasma membrane-localized aquaporin-family transporters in blue hydrangea sepals of aluminum hyperaccumulating plant. **PLoS one**, v. 7, n. 8, e43189, 2012.

NEGISHI, Takashi et al. Plasma membrane-localized A l-transporter from blue hydrangea sepals is a member of the anion permease family. **Genes to Cells**, v. 18, n. 5, p. 341-352, 2013.

OSATO, Yasue; YOKOYAMA, Ryusuke; NISHITANI, Kazuhiko. A principal role for AtXTH18 in Arabidopsis thaliana root growth: a functional analysis using RNAi plants. **Journal of plant research**, v. 119, n. 2, p. 153-162, 2006.

OWINO-GERROH, C.; GASCHO, G. J. Effect of silicon on low pH soil phosphorus sorption and on uptake and growth of maize. **Communications in soil science and plant analysis**, v. 35, n. 15-16, p. 2369-2378, 2005.

PAREDEZ, Alexander R.; SOMERVILLE, Christopher R.; EHRHARDT, David W. Visualization of cellulose synthase demonstrates functional association with microtubules. **Science**, v. 312, n. 5779, p. 1491-1495, 2006.

PARKER, Charlotte C. et al. Pectin distribution at the surface of potato parenchyma cells in relation to cell− cell adhesion. **Journal of agricultural and food chemistry**, v. 49, n. 9, p. 4364-4371, 2001.

PATI, Sajal et al. Effect of silicon fertilization on growth, yield, and nutrient uptake of rice. **Communications in Soil Science and Plant Analysis**, v. 47, n. 3, p. 284-290, 2016.

PETERSEN, Pia Damm et al. Engineering of plants with improved properties as biofuels feedstocks by vessel-specific complementation of xylan biosynthesis mutants. **Biotechnology for Biofuels**, v. 5, n. 1, p. 1-19, 2012.

RAHMAN, Taj Ur et al. Spectroscopic and density functional theory studies of 7-hydroxy-3′-methoxyisoflavone: a new isoflavone from the seeds of Indigofera heterantha (Wall). **Spectrochimica Acta Part A: Molecular and Biomolecular Spectroscopy**, v. 148, p. 375-381, 2015.

RAMMOHAN, Aluru et al. In silico, in vitro antioxidant and density functional theory based structure activity relationship studies of plant polyphenolics as prominent natural antioxidants. **Arabian Journal of Chemistry**, v. 13, n. 2, p. 3690-3701, 2020.

SASAKI, Masao; YAMAMOTO, Yoko; MATSUMOTO, Hideaki. Lignin deposition induced by aluminum in wheat (Triticum aestivum) roots. **Physiologia Plantarum**, v. 96, n. 2, p. 193-198, 1996.

SHAKI, Hosien et al. Modeling the interaction between anti-cancer drug penicillamine and pristine and functionalized carbon nanotubes for medical applications: density functional theory investigation and a molecular dynamics simulation. **Journal of Biomolecular Structure and Dynamics**, 2019.

SHARMA, Pallavi; DUBEY, R. S. Involvement of oxidative stress and role of antioxidative defense system in growing rice seedlings exposed to toxic concentrations of aluminum. **Plant cell reports**, v. 26, n. 11, p. 2027-2038, 2007.

SHUKLA, P. K.; MISHRA, P. C. DNA lesions caused by ROS and RNOS: A review of interactions and reactions involving guanine. **Practical Aspects of Computational Chemistry**, p. 415-443, 2009.

SIVAGURU, Mayandi et al. Aluminum rapidly depolymerizes cortical microtubules and depolarizes the plasma membrane: evidence that these responses are mediated by a glutamate receptor. **Plant and Cell Physiology**, v. 44, n. 7, p. 667-675, 2003.

SUJKOWSKA-RYBKOWSKA, Marzena; BORUCKI, Wojciech. Pectins esterification in the apoplast of aluminum-treated pea root nodules. **Journal of plant physiology**, v. 184, p. 1-7, 2015.

SWAIN, C.; CHAINY, G. B. N. Aluminum effect on lipid peroxidation and on the activities of superoxide dismutase and catalase in the cerebral hemisphere and liver of young chicks. **Journal of trace elements in medicine and biology**, v. 11, n. 2, p. 77-82,

TAHARA, Ko et al. Identification of a hydrolyzable tannin, oenothein B, as an aluminum-detoxifying ligand in a highly aluminum-resistant tree, Eucalyptus camaldulensis. **Plant physiology**, v. 164, n. 2, p. 683-693, 2014.

TANG, X. et al. Poplar PdMYB221 is involved in the direct and indirect regulation of secondary wall biosynthesis during wood formation. **Scientific reports**, v. 5, p. 1–14, 2015.

TERAOKA, Tsuyoshi et al. Aluminum rapidly inhibits cellulose synthesis in roots of barley and wheat seedlings. **Journal of Plant Physiology**, v. 159, n. 1, p. 17-23, 2002.

VERHERTBRUGGEN, Yves et al. An extended set of monoclonal antibodies to pectic homogalacturonan. **Carbohydrate research**, v. 344, n. 14, p. 1858-1862, 2009.

VERHERTBRUGGEN, Yves et al. Mannan synthase activity in the CSLD family. **Plant signaling & behavior**, v. 6, n. 10, p. 1620-1623, 2011.

VERHERTBRUGGEN, Yves et al. The TaCslA12 gene expressed in the wheat grain endosperm synthesizes wheat-like mannan when expressed in yeast and Arabidopsis. **Plant Science**, v. 302, p. 110693, 2021.

VO, Quan V. et al. Density functional theory study of the role of benzylic hydrogen atoms in the antioxidant properties of lignans. **Scientific reports**, v. 8, n. 1, p. 1-10, 2018.

VOINICIUC, Cătălin et al. MUCILAGE-RELATED10 produces galactoglucomannan that maintains pectin and cellulose architecture in Arabidopsis seed mucilage. **Plant Physiology**, v. 169, n. 1, p. 403-420, 2015.

VOXEUR, Aline; HÖFTE, Herman. Cell wall integrity signaling in plants:“To grow or not to grow that's the question”. **Glycobiology**, v. 26, n. 9, p. 950-960, 2016.

WANG, Huai et al. The origin of the naked grains of maize. **Nature**, v. 436, n. 7051, p. 714-719, 2005.

WANG, Yuqi et al. NIP1; 2 is a plasma membrane-localized transporter mediating aluminum uptake, translocation, and tolerance in Arabidopsis. **Proceedings of the National Academy of Sciences**, v. 114, n. 19, p. 5047-5052, 2017.

WI, S. G. et al. The pattern of distribution of pectin, peroxidase and lignin in the middle lamella of secondary xylem fibres in alfalfa (Medicago sativa). **Annals of Botany**, v. 95, n. 5, p. 863-868, 2005.

XIA, Jixing et al. Plasma membrane-localized transporter for aluminum in rice. **Proceedings of the National Academy of Sciences**, v. 107, n. 43, p. 18381-18385, 2010.

XIA, Jixing; YAMAJI, Naoki; MA, Jian Feng. A plasma membrane-localized small peptide is involved in rice aluminum tolerance. **The Plant Journal**, v. 76, n. 2, p. 345-355, 2013.

Yamamoto Y, Kobayashi Y, Matsumoto H. 2001. Lipid peroxidation is an early symptom triggered by aluminum, but not the primary cause of elongation inhibition in pea roots. **Plant Physiol**. 125:199–208

YAN, Guochao et al. Silicon alleviates salt stress-induced potassium deficiency by promoting potassium uptake and translocation in rice (Oryza sativa L.). **Journal of Plant Physiology**, v. 258, p. 153379, 2021.

YANG, Jian Li et al. Cell wall polysaccharides are specifically involved in the exclusion of aluminum from the rice root apex. **Plant Physiology**, v. 146, n. 2, p. 602-611, 2008.

YANG, Jian Li et al. PtoMYB156 is involved in negative regulation of phenylpropanoid metabolism and secondary cell wall biosynthesis during wood formation in poplar. **Scientific reports**, v. 7, n. 1, p. 1-14, 2017.

ZHU, Xiao Fang et al. Elevated carbon dioxide alleviates aluminum toxicity by decreasing cell wall hemicellulose in rice (Oryza sativa). **Frontiers in physiology**, v. 8, p. 512, 2017.

.